Dynamic traffic assignment with a node-based cell transmission model satisfying the link-level first-in-first-out principle

Sai Kiran Mayakuntla[1], Ashish Verma[2]

Abstract:

This paper develops node-based formulations for user equilibrium (UE) and system optimum (SO) dynamic traffic assignment (DTA) problems with departure time choice and route choices for general multiple origin-destination networks. Both the formulations are embedded with a new cell transmission model that satisfies the link-level First-In-First-Out (FIFO) principle. Because the formulations are node-based, the need for path enumeration is obviated, which results in considerable computational efficiency compared to the existing path-based models. While this advantage of node-based (or bush-based) models has been widely accepted in the literature of static traffic assignment, the formulations of dynamic traffic assignment models have thus far been path-based. The present work first describes a node-based cell transmission model that satisfies the link-level FIFO principle, which is fit within a DTA framework that facilitates efficient computation of UE and SO solutions. Further contributions of the work include the introduction of a backpropagation algorithm to efficiently compute marginal costs and complementarity formulations of the problems. Finally, numerical results are presented to demonstrate the performance of the proposed models using two standard test networks, along with a discussion of their convergence.

Introduction:

There are broadly two types of dynamic traffic assignment (DTA) problems: (1) user equilibrium DTA (UE-DTA) and (2) system optimal DTA (SO-DTA). In a UE-DTA, the individual travel costs of the drivers on the road network are minimized by their travel choices and they have no incentive to change them. By contrast, in a SO-DTA, the travel choices are made such that the total travel cost of the system is minimized. The solutions to the two problems provide useful insights into the quality and efficiency of transportation networks, and they have been extensively studied not only as isolated problems (Merchant & Nemhauser, 1978; Ziliaskopoulos, 2000; Ramadurai, et al., 2010), but as sub-problems within applications such as

1

Research Scholar, Department of Civil Engineering, Indian Institute of Science (IISc), Bangalore-560012, India. E-mail: mayakuntlasaikiran@gmail.com.

2

Associate Professor, Department of Civil Engineering and Centre for Infrastructure, Sustainable Transport, and Urban Planning (CiSTUP), Indian Institute of Science (IISc), Bangalore-560012, India. E-mail: ashishv@civil.iisc.ernet.in

evacuation planning (Shen et al., 2006), congestion pricing (Arnott et al., 1993; Shen & Zhang, 2009), network design (Karoonsoontawong & Waller, 2010), etc.

Any DTA model relies on a core module known as dynamic network loading (DNL), which includes rules for flow propagation, conservation and the estimation of travel times. Of the many such DNL models used in the past, cell transmission models (CTM) have been quite popular due to their ability to reproduce realistic, spatio-temporal phenomena like shockwave propagation and queue spillbacks. CTMs are typically embedded within the DTA models and optimization problems are formulated to obtain the user equilibrium and system optimal solutions. Some such formulations have resulted in the violation of the first-in-first-out (FIFO) principle, which must be satisfied by any realistic traffic flow model. It has also been observed that some of these models exhibit an artificial holding back of the traffic despite the availability of space downstream (Doan & Ukkusuri, 2012). Some recent works have addressed both these issues by using CTM as an implicit simulation method and formulating the variational inequality (VI) based models for the DTA problems. These include Szeto & Lo (2004), where both the route and departure time choices are incorporated in the model for a general network with elastic demand. Similarly, Han et al. (2011) formulated the UE-DTA problem within the framework of complementarity theory for a network with a single origin-destination (O-D) pair and multiple user classes with elastic demand. This work is extended for multiple O-D pairs by Ukkusuri et al. (2012) with maximum and average travel time models and a heuristic solution procedure based on the projection algorithm from the VI theory. Recently, Doan & Ukkusuri (2015) developed a similar SO-DTA formulation for general multi-OD networks with both route and departure time choices and they also provided an estimation procedure for path marginal costs that accurately captures the effect of any perturbation on all other traffic. However, all these models are path-based, i.e., the path choices are made by the traffic at the time of their entry into the network, and it has been acknowledged that considerable computational complexity arises from the path enumeration (Doan & Ukkusuri, 2015). While it has long been accepted in the case of static traffic assignment (STA) that node-based (or bush-based) models are computationally efficient than path-based ones and extensive literature is available on node-based STA models (Bar-Gera, 2002; Nie, 2010; Gentile, 2012), the same is surprisingly lacking in the case of DTA problems, possibly because of the difficulty of tractable formulation of such models.

The present work proposes node-based formulations for the UE-DTA & SO-DTA problems that incorporate many important features of the previous models like multiple O-D pairs, departure time choices and route choices, while avoiding their drawbacks such as holding back problem and FIFO violation. Since the models are node-based, the route choices are determined by the turning choices made by the traffic at diverging intersections, if and when they reach them. The CTM embedded within these formulations satisfies FIFO level 3 (or) link-level FIFO, as defined by Carey et al. (2014). While Carey et al. (2014) does provide algorithms for the implementation of such a CTM, an alternative implementation is devised in the present study to facilitate various computations of the DTA problems, including a backpropagation algorithm that can calculate all the relevant marginal costs with about the same computational complexity as a single simulation run. The proofs of the solution existence and some of the solution procedures of the proposed formulations given here are based on the techniques introduced in the earlier studies by Han et al. (2011), Ukkusuri et al. (2012) and Doan & Ukkusuri (2015).

In the following section, a Cell Transmission Model (CTM) is presented for a general network with demands between multiple O-D pairs incorporating the departure time choices for each O-D pair and the time-dependent turning choices at each diverging intersection. Further, detailed algorithms are given for the flow computations at merging and diverging intersections. This is followed by the derivation of recursive equations for average travel costs from the entrance of each link towards each destination and a backpropagation algorithm is described to calculate the marginal costs with respect to all the choice variables. Next, the DUE problem with the proposed CTM embedded in it is formulated as a complementarity problem, whereas the DSO problem is presented as an optimization problem. The existence of the DUE solution is then briefly discussed using the complementarity and variational inequality theory, followed by the presentation of a solution algorithm that can be adapted for both the problems and a discussion of numerical experiments demonstrating the application of the proposed formulations. And the paper concludes with a brief summary of the present work and a note on the scope for further work.

Notation:

Indices:

i, j, k - Indices for cells
s - Index for destination cells
t, t', τ, τ' - Indices for timesteps
l, l' - Indices for links

Parameters:

T_m - Maximum departure time
T - Maximum time horizon
Q^i - Flow capacity into and out of cell i
N^i - Jam density of cell i
δ^i - Congestion wave parameter of cell i
n_i - Number of cells between the cell i and the entry cell of the link it belongs to, inclusive of both.
α^s - Unit cost of travel time for traffic destined to s
β^s - Unit cost of early arrival for traffic destined to s
γ^s - Unit cost of late arrival for traffic destined to s
ε, δ - Infinitesimal parameter used to create modified cumulative curves
D_s^i - Total demand from a source cell i to a sink cell s
M - Penalty value for the traffic that fails to reach its destination by the end of the simulation
λ - Learning rate in the projection algorithm

Sets:

C - Set of all cells

C_O - Set of ordinary cells
C_R - Set of source cells
C_S - Set of sink cells
C_D - Set of diverging cells
C_M - Set of merging cells
C_l - Set of all cells on link l
L - Set of all links
$en(l)$ - Entry cell of link l
$ex(l)$ - Exit cell of link l
Γ_i - Set of all immediate downstream cells of a cell i
Γ_i^{-1} - Set of all immediate upstream cells of a cell i
X_l - Set of all immediate downstream links of a link l
X_l^{-1} - Set of all immediate upstream links of a link l

Variables:

$x_{s,t}^{i}$ - Occupancy of cell i at time t by the traffic destined to the sink cell s
$y_{s,t}^{i,j}$ - Flow destined to the sink cell s from cell i to cell j at time t
$y_{s,t}^{i\cdot}$ - Outflow from cell i of the traffic destined to the sink cell s at timestep t
$y_{s,t}^{\cdot i}$ - Inflow to cell i of the traffic destined to the sink cell s at timestep t
$y_{\cdot t}^{i\cdot}$ - Total outflow from cell i at timestep t
$y_{\cdot t}^{\cdot i}$ - Total inflow to cell i at timestep t
$\bar{y}_{s,t}^{i,j}$ - Cumulative sum variable corresponding to $y_{s,t}^{i,j}$
$\bar{y}_{s,t}^{i\cdot}$ - Cumulative sum variable corresponding to $y_{s,t}^{i\cdot}$
$\bar{y}_{s,t}^{\cdot i}$ - Cumulative sum variable corresponding to $y_{s,t}^{\cdot i}$
$\bar{y}_{\cdot t}^{i\cdot}$ - Cumulative sum variable corresponding to $y_{\cdot t}^{i\cdot}$
$\bar{y}_{\cdot t}^{\cdot i}$ - Cumulative sum variable corresponding to $y_{\cdot t}^{\cdot i}$
$\tilde{y}_{\cdot t}^{i\cdot}$ - Auxiliary variable corresponding to $\bar{y}_{\cdot t}^{i\cdot}$
$\tilde{y}_{\cdot t}^{\cdot i}$ - Auxiliary variable corresponding to $\bar{y}_{\cdot t}^{\cdot i}$
$r_{s,t}^{i}$ - Proportion of demand from the source cell i to destination cell s that enters the system at time t
$d_{s,t}^{i,j}$ - Proportion of traffic destined to s in a diverging cell i at timestep t that chooses to move into an immediate downstream cell j
$A_t^{l,i}$ - Time of entry into link l of the earliest vehicles exiting cell i at time t
$a_\tau^{l,i}$ - Time of exit from cell i of the earliest vehicles entering a link l at time τ
$z_{\tau,t}^{l,i}$ - Proportion of vehicles that enter a link l at time t and exit cell i at time τ
$\hat{z}_{\tau,t}^{l,i}$ - Auxiliary variable corresponding to $z_{\tau,t}^{l,i}$
$Z_{s,\tau,t}^{l\cdot}$ - Proportion of traffic destined to s that enters the link l in timestep τ and exits in timestep t
$Z_{s,\tau,t}^{l,l'}$ - Proportion of traffic destined to s that enters the link l in timestep τ and exits in timestep t to enter a downstream link l'

$p_{s,\tau,t}^{l}$ - Proportion of traffic that enters the link l in timestep τ and reaches its destination in timestep t
$TT_{s,\tau}^{l}$ - Expected travel time of the traffic destined to s that enters the link l in timestep τ
$e_{s,\tau}^{l}$ - Expected early arrival costs of the traffic destined to s that enters the link l in timestep τ
$f_{s,\tau}^{l}$ - Expected late arrival costs of the traffic destined to s that enters the link l in timestep τ
$TC_{s,\tau}^{l}$ - Expected travel cost of the traffic destined to s that enters the link l in timestep τ
TSC - Total system cost

Cell transmission model:

Extensions of Cell transmission model (Daganzo, 1994; Daganzo, 1995) have been widely used as dynamic network loading (DNL) models due to their ability to accurately capture spatio-temporal phenomena like shockwaves and queue spillbacks. Unless the overtaking behavior is explicitly included, these models typically ensure FIFO behavior, in order to avoid arbitrary, unrealistic behavior that could arise otherwise. Carey et al. (2014) defined three levels of FIFO approximations and presented algorithms for CTMs that satisfy each of them. In this section, an alternative implementation of CTM that satisfies FIFO level 3, i.e., link-level FIFO behavior, is presented. This will facilitate the computations performed to solve the node-based DTA problems detailed in later sections. Given the departure time choices at each source and the turning choices at each diverging intersection, the CTM presented in this section uniquely determines the cell flows and occupancies on a multiple O-D network for the time period considered. Vehicles are labeled by their destinations (or sink cells) and their paths are determined by the turning choices made at diverging intersections. This obviates the need to enumerate all the paths between each O-D pair, which significantly reduces the computational cost of the model.

Table 1: Possible cell types in the model

Cell type	No. of outgoing connectors ($\lvert\boldsymbol{\Gamma_i}\rvert$)	No. of Incoming connectors ($\lvert\boldsymbol{\Gamma_i^{-1}}\rvert$)
Ordinary (C_O)	1	1
Merging (C_M)	1	>1
Diverging (C_D)	>1	1
Sink (C_S)	0	1
Source (C_R)	1	0

a) Cell updates:

$$x^{i}_{s,0} = 0 \qquad \forall i \ \in C;\ d \ \in C_S \qquad (1)$$

$$x^{i}_{s,t} = x^{i}_{s,t-1} - y^{i.}_{s,t-1} + y^{i.}_{s,t-1} \qquad \forall i \in C; s \in C_S; t \in \{1, \dots, T\} \qquad (2)$$

$$y^{i.}_{s,t} = \sum{}_{j \in \Gamma_i} y^{i,j}_{s,t} \qquad \forall i \in C - C_S; s \in C_S; t \in \{1, \dots, T\} \qquad (3)$$

$$y^{.i}_{s,t} = \sum{}_{j \in \Gamma_i^{-1}} y^{i,j}_{s,t} \qquad \forall i \in C - C_R; s \in C_S; t \in \{1, \dots, T\} \qquad (4)$$

$$y^{i.}_{s,t} = 0 \qquad \forall i \in C_S; s \in C_S; t \in \{1, \dots, T\} \qquad (5)$$

$$y^{.i}_{s,t} = r^{i}_{s,t} \times D^{i}_{s} \qquad \forall i \in C_R; s \in C_S; t \in \{1, \dots, T\} \qquad (6)$$

$$r^{i}_{s,t} = 0 \qquad \forall t \in \{T_m + 1, \dots, T\}; i \in C_R; s \in C_S \qquad (7)$$

$$\sum\nolimits_{t=0}^{T_m} r^{i}_{s,t} = 1 \qquad \forall i \in C_R; s \in C_S \qquad (8)$$

$$x^{i}_{.t} = \sum\nolimits_{s \,\in\, C_S} x^{i}_{s,t} \qquad \forall i \ \in C;\ t \in \{1, \dots, T\} \qquad (9)$$

$$y^{.i}_{.t} = \sum\nolimits_{s \in C_S} y^{.i}_{s,t} \qquad \forall i \in C; t \in \{1, \dots, T\} \qquad (10)$$

$$y^{i.}_{.t} = \sum\nolimits_{s \in C_S} y^{i.}_{s,t} \qquad \forall i \in C; t \in \{1, \dots, T\} \qquad (11)$$

$$x^{i}_{.t} = x^{i}_{.t-1} - y^{i.}_{.t-1} + y^{.i}_{.t-1} \qquad \forall i \in C; t \in \{1, \dots, T\} \qquad (12)$$

The applicability of the above equations to a given cell in the cell transmission network depends on its type, as defined in table 1. Cells with multiple incoming and outgoing connectors are disallowed in the present model, as is common in the existing CTM literature. Eqs. (1)-(8) give the basic cell update equations disaggregated by the destinations. Eq. (1) ensures that all cells are empty at the beginning of the simulation. Eq. (2) updates the destination-wise occupancies in each cell. Eqs. (3) & (5) and eqs. (4) & (6) provide the outflows and inflows, respectively, of all the cells in the network. Sink cells are assumed to have infinite store capacity and all the vehicles entering them remain there till the end of the simulation. Similarly, inflows to source cells depend on the departure time choices at those cells. Eq. (8) ensures that the demand at each source enters the network before the maximum departure time, and eq. (7) ensures no vehicles are entering after that. Eqs. (9), (10) & (11) give the aggregated cell occupancies, inflows and outflows, respectively. And eq. (12) is the aggregate occupancy update equation that can be derived from the equations above it.

It may be useful to clarify certain terms before moving further. Unlike some previous studies (Ukkusuri et al., 2012; Doan et al., 2015), the terms “link” and “connector” have been used with two different meanings here. A “connector” refers to the abstract representation of the allowability of flow between any two given cells. There are three possible types of connectors in the present model: ordinary, which joins a cell with a single outgoing connector to another cell with a single incoming connector; merging, which joins a cell with a single outgoing connector to a merging cell; and diverging, which joins a diverging cell to another cell with a single incoming connector. A “link” can be defined as a maximal contiguous sequence of cells joined by ordinary connectors. In the following subsection, flows on the three types of equations are computed in such a way that the link-level FIFO is satisfied by the model.

b) Flow computations:

In the implementation algorithm of FIFO level 3 described by Carey et al. (2014), vehicle cohorts are labeled by their route and time of entry into a given link, and the disaggregated cell updates are performed by keeping track of the position of these cohorts along the link. In contrast, labeling is done here by the vehicle destinations and their entry times and their disaggregation at each cell is performed using cumulative flows. However, as observed in Nie (2003), such usage of cumulative flows gives rise to difficulties, as they are not strictly increasing and remain flat at portions with zero flow. This could occur due to two major factors: (a) A temporary inflow drop to zero (e.g., during light traffic), and (b) A temporary outflow capacity drop to zero (e.g., during a red phase). Nie (2003) circumvented this problem by estimating the link travel times in the zero-flow portions through the method of linear interpolation. Alternatively, Long et al. (2011) dealt with the same issue by adding small, non-zero values to the cumulative flows at every timestep and essentially forcing them to become strictly increasing. In the present work, a limit-based approach is used to derive conditional formulas that can estimate the required values using non-decreasing cumulative flow curves. More specifically, the cumulative entry flows to each link (eq. 13) and the cumulative exit flows out of each cell (eq. 14) are modified by adding a small, positive constant value ($\varepsilon > 0$) at each timestep and defining some new terms as the limits of functions using these modified curves as the constant value approaches zero.

$$\tilde{y}_{.t}^{.en(l)} = \bar{y}_{.t}^{.en(l)} + (t+1) \times \varepsilon, \quad \forall l \in L; t \in \{0, \dots, T-1\}, \tag{13}$$

$$\tilde{y}_{.t}^{i.} = \begin{cases} \bar{y}_{.t}^{i.} \; (= 0) & if\ t < n_i \\ \bar{y}_{.t}^{i.} + (t - n_i + 1) \times \varepsilon & o/w \end{cases}, \quad \forall l \in L; t \in \{0, \dots, T-1\}. \tag{14}$$

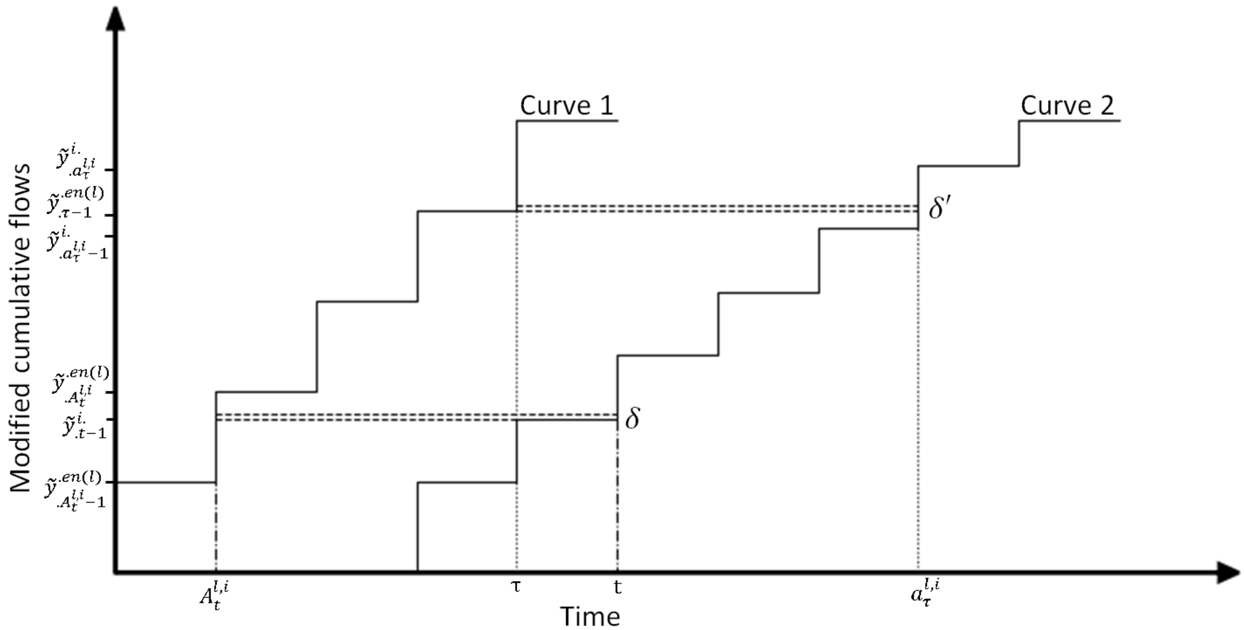

Figure 1: Illustration of definitions 1 & 2. Curves 1 & 2 represent the modified cumulative curves (eqs. 13-14) of the flows entering a given link l and those exiting a cell i on that link, respectively. For traffic flow satisfying FIFO level 3, the earliest δ (> 0) vehicles exiting cell i at time t must have entered the link at $A_t^{l,i}$, and the earliest δ' (> 0) vehicles entering the link at time τ must exit the cell i at time $a_\tau^{l,i}$.

Definition 1: The time of entry of the earliest vehicles exiting cell i at time t is given by:

$$A_t^{l,i} = \begin{cases} -1 & if\ t < n_i \\ \lim_{\varepsilon \to 0^+} \lim_{\delta \to 0^+} max\left\{t' | \tilde{y}_{.t-1}^{i.} + \delta > \tilde{y}_{.t'-1}^{.en(l)}\right\} & o/w \end{cases}, \quad \forall i \in C_l; l \in L; t \in \{0, \dots, T-1\}. \ (15)$$

To understand the above definition, first observe that n_i is the number of cells between the entry cell of link l and cell i, inclusive of both. Under free-flow conditions, the outflow from any given cell must be equal to its occupancy, as vehicles move at a speed of one cell per timestep, which makes n_i the minimum number of timesteps in which a vehicle cohort entering a link l can begin exiting cell i. Since the entire network is empty at the beginning of our simulation, there cannot be any outflow from cell i before n_i, where a value of -1 is assigned to indicate this. Further the modifications made to the cumulative flows are equivalent to increasing all the relevant parameters of the cells, i.e., flow and storage capacities, and the demand from the incoming links by ε. In eq. (15), δ represents vehicles exiting cell i at the beginning of the timestep t. Figure 1 may further clarify the definition.

Proposition 1: $A_t^{l,i} = \begin{cases} -1 & if\ t < n_i \\ \lim_{\varepsilon \to 0^+} max\left\{t' | \tilde{y}_{.t-1}^{i.} \geq \tilde{y}_{.t'-1}^{.en(l)}\right\} \end{cases} \quad \forall i \in C_l; l \in L; t \in \{0, \dots, T-1\}. \qquad (16)$

Proof: This result can easily be verified using eq. (15). □

Proposition 2:

(i) For all $\tau < t - n_i$ and $\varepsilon > 0$,
a) $\bar{y}_{.t}^{i.} > \bar{y}_{.\tau}^{.en(l)} \Rightarrow \tilde{y}_{.t}^{i.} > \tilde{y}_{.\tau}^{.en(l)}$
b) $\bar{y}_{.t}^{i.} = \bar{y}_{.\tau}^{.en(l)} \Rightarrow \tilde{y}_{.t}^{i.} > \tilde{y}_{.\tau}^{.en(l)}$
c) $\bar{y}_{.t}^{i.} < \bar{y}_{.\tau}^{.en(l)} \Rightarrow \tilde{y}_{.t}^{i.} < \tilde{y}_{.\tau}^{.en(l)}, \quad \forall \varepsilon < \frac{\bar{y}_{.\tau}^{.en(l)} - \bar{y}_{.t}^{i.}}{t - n_i}$

(ii) For all $\tau = t - n_i$ and $\varepsilon > 0$,
(a) $\bar{y}_{.t}^{i.} > \bar{y}_{.\tau}^{.en(l)} \Rightarrow \tilde{y}_{.t}^{i.} > \tilde{y}_{.\tau}^{.en(l)}$
(b) $\bar{y}_{.t}^{i.} = \bar{y}_{.\tau}^{.en(l)} \Rightarrow \tilde{y}_{.t}^{i.} = \tilde{y}_{.\tau}^{.en(l)}$
(c) $\bar{y}_{.t}^{i.} < \bar{y}_{.\tau}^{.en(l)} \Rightarrow \tilde{y}_{.t}^{i.} < \tilde{y}_{.\tau}^{.en(l)}$

(iii) For all $\tau > t - n_i$ and $\varepsilon > 0$,
(a) $\bar{y}_{.t}^{i.} = \bar{y}_{.\tau}^{.en(l)} \Rightarrow \tilde{y}_{.t}^{i.} < \tilde{y}_{.\tau}^{.en(l)}$
(b) $\bar{y}_{.t}^{i.} < \bar{y}_{.\tau}^{.en(l)} \Rightarrow \tilde{y}_{.t}^{i.} < \tilde{y}_{.\tau}^{.en(l)}$

$$\forall\, i \in C - C_S; t \in \{n_i, \dots, T-1\}; \tau \in \{0, \dots, T - n_i - 1\}. \tag{17}$$

Proof: All the statements in eq. (17) can be verified using definitions of the modified cumulative flows in eqs. (13) & (14). □

Corollary 1: $\bar{y}_{.t}^{i.} \leq \bar{y}_{.t-n_i}^{.en(l)} \quad \forall i \in C_l; l \in L; t \in \{n_i, \dots, T-1\}.$ (18)

This corollary says that no vehicle entering a link later than $t - n_i$ can exit the cell i before $t + 1$.

Corollary 2: $\tilde{y}_{.t}^{i.} = \tilde{y}_{.\tau}^{.en(l)}$, iff $\tau = t - n_i$ & $\bar{y}_{.t}^{i.} = \bar{y}_{.\tau}^{.en(l)}$, $\quad \forall i \in C_l; l \in L; \tau \in \{0, \dots, T-1\}.$ (19)

Proposition 3: $A_t^{l,i} \leq t - n_i, \quad \forall i \in C_l;\ l \in L;\ t \in \{n_i, \dots, T-1\}.$ (20)

Proof: As we assumed that the cell network is empty at the beginning of the simulation (eq. 1) and all non-sink cells must have a non-zero outflow capacity, the earliest vehicles entering the link l at time 0 must move at their free-flow speed, making eq. (19) true at $t = n_i$. For $t > n_i$, eq. (20) can be verified to be true using eqs. (15) & (17). □

Proposition 4: $A_t^{l,i} = \begin{cases} -1 & if\ t < n_i \\ t - n_i & if\ t \geq n_i\ and\ \bar{y}_{.t-1}^{i.} = \bar{y}_{.t-n_i-1}^{.en(l)}, \\ max\left\{t' \middle| \bar{y}_{.t-1}^{i.} \geq \bar{y}_{.t'-1}^{.en(l)}\right\} & o/w \end{cases} \quad \forall i \in C_l;\ l \in L;\ t \in \{0, \dots, T-1\}.$

(21)

Proof: Since $A_t^{l,i}$ can utmost be equal to $t - n_i$ (eq. (20)), eq. (21) is verified below only with cases subdividing $\tau \leq t - n_i$.

Case (i): $\bar{y}_{.t-1}^{i.} = \bar{y}_{.t-n_i-1}^{.en(l)}$

From eq. (17), $\tilde{y}^{.en(l)}_{.t-n_i-1} = \tilde{y}^{.en(l)}_{.t-1} < \tilde{y}^{.en(l)}_{.t-n_i}, \quad \forall \varepsilon > 0$. Therefore, from eq. (16), $A^{l,i}_t = t - n_i$.

Case (ii): $\bar{y}^{.en(l)}_{.\tau-1} < \bar{y}^{i.}_{.t-1} < \bar{y}^{.en(l)}_{.\tau}$

Again from eqs. (17) & (16), this implies $\tilde{y}^{.en(l)}_{.t-n_i-1} < \tilde{y}^{.en(l)}_{.t-1} < \tilde{y}^{.en(l)}_{.t-n_i}$ and $A^{l,i}_t = \tau$.

Case (iii): $\bar{y}^{.en(l)}_{.\tau-m-1} = \bar{y}^{i.}_{.t-1} < \bar{y}^{.en(l)}_{.\tau}, \quad where\ m \geq 0$

If $m > 0$, since the cumulative flows are non-decreasing, $\bar{y}^{.en(l)}_{.\tau-m-1} = \bar{y}^{.en(l)}_{.\tau-1}$. Therefore, from eq. (17), $\tilde{y}^{.en(l)}_{.\tau-m-1} < \tilde{y}^{.en(l)}_{.\tau-1} < \tilde{y}^{i.}_{.t-1} < \tilde{y}^{.en(l)}_{.\tau}, \quad \forall \varepsilon < \frac{\bar{y}^{.en(l)}_{.\tau} - \bar{y}^{i.}_{.t}}{t-n_i}$. Thus, $A^{l,i}_t = \tau$.

Eq. (21) follows after combing the results from the above three cases. □

Next, an inverse notion to $A^{l,i}_t$ is introduced that will also be useful in later computations.

Definition 2: The time of exit from cell i of the earliest vehicles entering a link l at time τ is given by:

$$a^{l,i}_\tau = \begin{cases} \lim_{\varepsilon \to 0^+} \lim_{\delta' \to 0^+} max\left\{\tau' | \tilde{y}^{.en(l)}_{.\tau-1} + \delta' > \tilde{y}^{i.}_{.\tau'-1}\right\} & if\ \tilde{y}^{.en(l)}_{.\tau-1} < \tilde{y}^{i.}_{.T-1}\ and\ \tau < T - n_i \\ T & o/w \end{cases}, \quad \forall i \in C_l;\ l \in L;\ \tau \in \{0, \dots, T-1\} \tag{22}$$

The first conditional is applicable to timesteps that do not entirely remain within the link l at the end of the simulation. A value of T is assigned to $a^{l,i}_\tau$ to the rest of the timesteps to indicate otherwise.

Proposition 5: $$a^{l,i}_\tau = \begin{cases} \lim_{\varepsilon \to 0^+} max\left\{\tau' | \tilde{y}^{.en(l)}_{.\tau-1} \geq \tilde{y}^{i.}_{.\tau'-1}\right\} & if\ \tilde{y}^{.en(l)}_{.\tau-1} < \tilde{y}^{i.}_{.T-1}\ and\ \tau < T - n_i \\ T & o/w \end{cases} \quad \forall i \in C_l;\ l \in L;\ \tau \in \{0, \dots, T-1\}. \tag{23}$$

Proposition 6: $a^{l,i}_\tau \geq \tau + n_i, \quad \forall i \in C_l;\ l \in L;\ \tau \in \{0, \dots, T - n_i - 1\}$. (24)

Proposition 7:

$$a^{l,i}_\tau = \begin{cases} \tau + n_i & if\ \bar{y}^{.en(l)}_{.\tau-1} = \bar{y}^{i.}_{.\tau+n_i-1}\ and\ \tau < T - n_i \\ max\left\{\tau' | \bar{y}^{.en(l)}_{.\tau-1} \geq \bar{y}^{i.}_{.\tau'-1}\right\} & if\ \bar{y}^{i.}_{.\tau+n_i-1} \neq \bar{y}^{.en(l)}_{.\tau-1} \leq \bar{y}^{i.}_{.T-1}\ and\ \tau < T - n_i \\ T & o/w \end{cases}, \quad \forall i \in C_l;\ l \in L;\ t \in \{0, \dots, T-1\}. \tag{25}$$

The proofs of the propositions 5, 6 & 7 are similar to those of 1, 3 & 4, respectively. Both the notions introduced above are clearly related and, in fact, the values of $a^{l,i}_\tau$ can directly be obtained using only $A^{l,i}_t$ values, without using cumulative flows.

Proposition 8: $a_\tau^{l,i} = \begin{cases} \tau + n_i & if\ \tau < T - n_i\ and\ A_{\tau+n_i}^{l,i} = \tau \\ min\{t | \tau \le A_{t+1}^{l,i}\}, & if\ \exists\ t \in \{n_i - 1, \dots, T-2\}\ s.t. \tau \le A_{t+1}^{l,i} \\ T & o/w \end{cases}$, $\forall i \in C_l;\ l \in L;\ t \in \{0, \dots, T-1\}$. (26)

Proof: Case (i): $\tau < T - n_i\ and\ A_{\tau+n_i}^{l,i} = \tau$

Let $t = \tau + n_i \ge n_i$. Then $\bar{y}_{.\tau-1}^{.en(l)} = \bar{y}_{.\tau+n_i-1}^{i.} \equiv \bar{y}_{.t-n_i-1}^{.en(l)} = \bar{y}_{.t-1}^{i.}$. Thus, from eq. (21), $a_\tau^{l,i} = \tau + n_i$.

Case (ii): $\bar{y}_{.\tau+n_i-1}^{i.} \ne \bar{y}_{.\tau-1}^{.en(l)} \le \bar{y}_{.T-1}^{i.}\ and\ \tau < T - n_i$

Again, let $t = \tau + n_i < T$. Then, $\bar{y}_{.t-1}^{i.} \ne \bar{y}_{.t-n_i-1}^{.en(l)} \le \bar{y}_{.T-1}^{i.}$. From eq. (21), this means that there exists $t \in \{n_i, \dots, T-1\}$ such that $\tau \le A_t^{l,i}$, which is equivalent to the second condition in eq. (26). The converse can be proven similarly.

Since in eqs. (16) & (25), $\tilde{y}_{.\tau-1}^{.en(l)} = \tilde{y}_{.\tau'-1}^{i.}$, if and only if $\tau' = \tau + n_i$ and $\bar{y}_{.\tau-1}^{.en(l)} = \bar{y}_{.\tau'-1}^{i.}$ (from eq. 19). This contradicts the above condition and can never occur in this case for any τ'. Now, let $a = min\{t | \tau \le A_{t+1}^{l,i}\}$.

$$\Rightarrow A_a^{l,i} < \tau \le A_{a+1}^{l,i}$$

From eq. (16), this implies

$$\tilde{y}_{.a-1}^{i.} < \tilde{y}_{.\tau-1}^{.en(l)} < \tilde{y}_{.a}^{i.}.$$

Thus, from eq. (23), $a_\tau^{l,i} = a$.

Case (iii): Since cases (i) & (ii) are equivalent to the first two conditionals in eq. (25), case (iii) must also be equivalent to its final conditional, which includes all the remaining possibilities. Therefore, here, $a_\tau^{l,i} = T$. □

Corollary 3: $a_t^{l,i} > t > A_t^{l,i}\quad \forall i \in C_l; l \in L; t \in \{0, \dots, T-1\}$. (27)

Proof: This result follows directly from eqs. (16), (20), (23) & (24). □

In a CTM satisfying FIFO level 3 (or) link-level FIFO, the vehicles exit each cell on the link in the same order as they entered it. But since the vehicles are only differentiated by their destinations, satisfying the FIFO principle here means appropriately calculating the outflow proportion bound to destination. The most obvious way to do that is by using linear interpolation as the outflow could be comprised of vehicles entering the link in multiple timesteps. To avoid introducing more cumbersome notation, an easily interpretable definition of those proportions is given below as a limit function of modified cumulative flows and $A_t^{l,i}$ values. Figure 2 provides an illustration of that definition by considering two main cases.

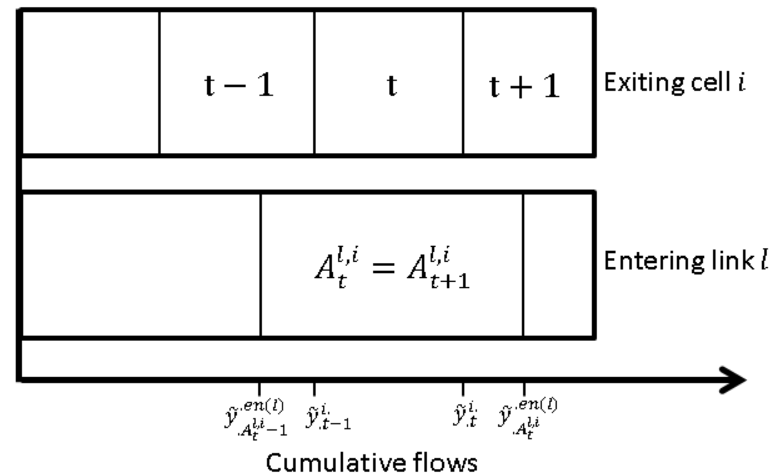

(a)

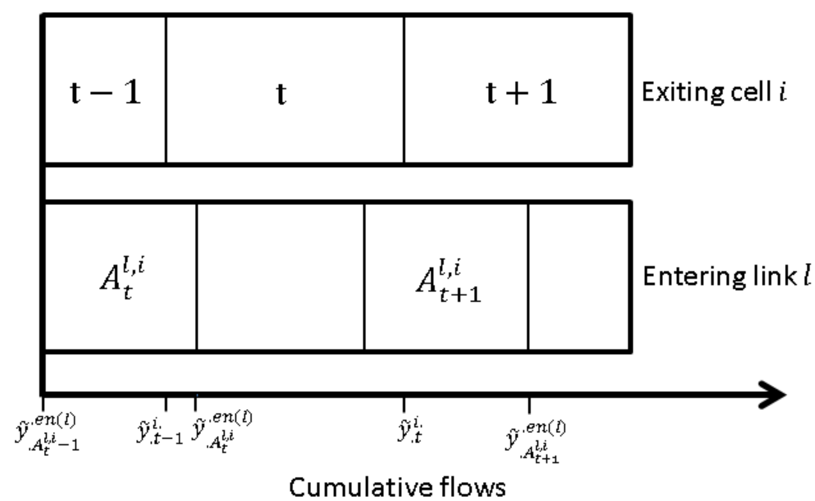

(b)

Figure 2: Illustration of definition 3. In case (a), all the vehicles exiting cell i at time t have entered the link l in a single timestep $A_t^{l,i}$ $(= A_{t+1}^{l,i})$, and it corresponds to the second conditional in eq. (28). Similarly, case (b) shows vehicles that entered in multiple timesteps exiting the cell at time t, which is related to the final three conditionals in eq. (28). Note that the free-flow condition would result in a special case of (b), where entry cohort exits in a single timestep but $A_t^{l,i} < A_{t+1}^{l,i}$.

Definition 3: The proportion of vehicles that enter a link l at time t and exit cell i at time τ $\left(z_{t,\tau}^{l,i}\right)$ is given by:

$$z_{\tau,t}^{l,i} = \lim_{\varepsilon \to 0^+} \hat{z}_{\tau,t}^{l,i}$$

where $\hat{z}_{\tau,t}^{l,i} = \begin{cases} 0 \quad if\ \tau < A_t^{l,i}\ or\ \tau > A_{t+1}^{l,i} \\ \frac{\tilde{y}_{.t}^{i.} - \tilde{y}_{.t-1}^{i.}}{\tilde{y}_{.\tau}^{.en(l)} - \tilde{y}_{.\tau-1}^{.en(l)}} \quad if\ A_t^{l,i} = \tau = A_{t+1}^{l,i} \\ \frac{\tilde{y}_{.\tau}^{.en(l)} - \tilde{y}_{.t-1}^{i.}}{\tilde{y}_{.\tau}^{.en(l)} - \tilde{y}_{.\tau-1}^{.en(l)}} \quad if\ A_t^{l,i} = \tau < A_{t+1}^{l,i} \\ 1 \quad if\ A_t^{l,i} < \tau < A_{t+1}^{l,i} \\ \frac{\tilde{y}_{.t}^{i.} - \tilde{y}_{.\tau-1}^{.en(l)}}{\tilde{y}_{.\tau}^{.en(l)} - \tilde{y}_{.\tau-1}^{.en(l)}} \quad if\ A_t^{l,i} < \tau = A_{t+1}^{l,i} \end{cases}.$ (28)

To understand the first conditional in the above equation, note that, under link-level FIFO, the earliest vehicles exiting cell i at time t have entered the link later than τ implies that the entry cohort of τ has completely exited the cell i before t. Similarly, if the earliest vehicles exiting cell i at time $t+1$ have entered the link earlier than τ, then the vehicles from τ must not have begun exiting cell i before $t+1$. Therefore, $z_{t,\tau}^{l,i}$ values must be zero for these two periods. The second conditional corresponds to a situation where all the vehicles exiting cell I at time t have come from the same entry cohort τ, whereas the other three conditionals combinedly represent the case where the cohort exits in multiple timesteps. An analogous definition could be given in terms of $a_\tau^{l,i}$ values, but it is instead derived from eq. (28) to demonstrate their consistency.

Proposition 9: $\hat{z}_{\tau,t}^{l,i}$ in eq. (28) can alternatively be given by:

$$\hat{z}_{\tau,t}^{l,i} = \begin{cases} 0 \quad if\ t < a_\tau^{l,i}\ or\ t > a_{\tau+1}^{l,i} \\ 1 \quad if\ a_\tau^{l,i} = t = a_{\tau+1}^{l,i} \\ \frac{\tilde{y}_{.t}^{i.} - \tilde{y}_{.\tau-1}^{.en(l)}}{\tilde{y}_{.\tau}^{.en(l)} - \tilde{y}_{.\tau-1}^{.en(l)}} \quad if\ a_\tau^{l,i} = t < a_{\tau+1}^{l,i} \\ \frac{\tilde{y}_{.t}^{i.} - \tilde{y}_{.t-1}^{i.}}{\tilde{y}_{.\tau}^{.en(l)} - \tilde{y}_{.\tau-1}^{.en(l)}} \quad if\ a_\tau^{l,i} < t < a_{\tau+1}^{l,i} \\ \frac{\tilde{y}_{.\tau}^{.en(l)} - \tilde{y}_{.t-1}^{i.}}{\tilde{y}_{.\tau}^{.en(l)} - \tilde{y}_{.\tau-1}^{.en(l)}} \quad if\ a_\tau^{l,i} < t = a_{\tau+1}^{l,i} \end{cases}. \qquad (29)$$

Proof: It can be seen that each conditional in eq. (29) has a corresponding equivalent conditional in eq. (28), which is verifiable using eq. (26). □

Proposition 10: $\sum_{t\in\{0,\dots,T-1\}} z_{\tau,t}^{l,i} = 1$, if and only if $\tau < T - n_i\ and\ a_{\tau+1}^{l,i} \le T-1$. (30)

Proof: This can again be easily verified using eqs. (25) & (29). □

Proposition 11: $\sum_{t'\in\{0,\dots,t\}} z_{\tau,t'}^{l,i} > 0 \Rightarrow \sum_{t'\in\{0,\dots,t\}} z_{\tau-1,t'}^{l,i} = 1, \quad \forall\ t \in \{1,\dots,T-1\}; \tau \in \{0,\dots,t-n_i\}.$
(31)

This proposition means that the vehicles entering a link at time $\tau - 1$ must have exited the cell i before the entry cohort of τ begins to exit. This can be derived using the eqs. (21) & (28).

Flow computations on the three types of connectors, i.e., ordinary, diverging and merging, can be performed now according to the methods given in Carey et al. (2014), but with the terms defined above. First, the aggregate flow from cell i to cell j through an ordinary connector at timestep t is given by:

$$y_{.t}^{i,j} = min\left(x_{.t}^{i}, Q^{i}, Q^{j}, \delta^{j}\left(N^{j} - x_{.t}^{j}\right)\right) \quad \forall (i,j) \in E_{O}; t \in \{0, \dots, T-1\}. \tag{32}$$

Similarly, at a merging intersection, the supply (or receiving capacity) of the merging cell is distributed among all its incoming cells based on some fixed proportions. In case the demand from an incoming cell is less than the supply allocated to it, the surplus is redistributed to the cells where the demand is greater. This iteration ends when either all the demands from the incoming cells are satisfied, or the supply is exhausted. This computation performed at each merging cell i and timestep t is presented in an algorithmic form below:

Initialize $y_{.t}^{k,i} = 0, \forall k \in \Gamma_{i}^{-1}; V = \Gamma_{i}^{-1}$;

$S_{k} = min\{x_{.t}^{k}, Q^{k}\};\ R_{k} = \frac{Q^{k}}{\sum_{k' \in \mathrm{I}} Q^{k'}} \times min\{Q^{i}, \delta^{i}\left(N^{i} - x_{.t}^{i}\right)\}, \forall\ k \in \mathrm{V}.$

while I is non-empty:

$U \leftarrow 0.$

for $k \in I$:

if $S_{k} \leq R_{k}$:

$y_{.t}^{k,i} = y_{.t}^{k,i} + S_{k};\ V = V - \{k\}.$

else $y_{.t}^{k,i} = y_{.t}^{k,i} + R_{k};\ U = U + S_{k} - R_{k}.$

for $k \in I$:

$S_{k} = S_{k} - R_{k};\ R_{k} = \frac{Q^{k}}{\sum_{k' \in \mathrm{I}} Q^{k'}} \times U.$

(33)

At any given timestep t, the proportion of inflow to each cell immediately downstream to a diverging cell is calculated using the destination-based turning choices at τ. The flow is calculated by considering the vehicle cohorts labeled by their entry times sequentially starting with the earliest vehicles remaining on link l at t, until either the sending capacity of the diverging cell or one of the receiving capacities its downstream cells is exhausted. In the latter case, traffic moving to the other downstream cells will be stuck behind that of the blocked one, which is a phenomenon often observed on real road intersections. Again, this method can be given in an algorithmic form as follows:

Initialize $y_{.t}^{i,j} = 0, \forall j \in \Gamma_{i}; h = A_{t}^{l,ex(l)}$.

$R_{j} = min\{Q^{j}, \delta^{j}\left(N^{j} - x_{.t}^{j}\right)\}, \forall j \in \Gamma_{i}$.

while $y_{.t}^{i,j} < R_{j}, \forall j \in \Gamma_{i}$ and $h \leq A_{t}^{l,ex(l)-1}$:

$$f = \begin{cases} \bar{y}_{.t-1}^{.ex(l)-1} - \bar{y}_{.t-1}^{.ex(l)} & if\ A_{t}^{l,ex(l)} = h = A_{t}^{l,ex(l)-1} \\ \bar{y}_{.h}^{.en(l)} - \bar{y}_{.t-1}^{.ex(l)}, & if\ A_{t}^{l,ex(l)} = h < A_{t}^{l,ex(l)-1} \\ y_{.h}^{.en(l)}, & if A_{t}^{l,ex(l)} < h < A_{t}^{l,ex(l)-1} \\ \bar{y}_{.t-1}^{.ex(l)-1} - \bar{y}_{.h-1}^{.en(l)}, & A_{t}^{l,ex(l)} < h = A_{t}^{l,ex(l)-1} \end{cases}$$

$$f_j = \begin{cases} 0 \quad if\ y_{.h}^{.en(l)} = 0 \\ f \times \sum_s \frac{y_{s,h}^{.en(l)}}{y_{.h}^{.en(l)}} \times d_{s,t}^{i,j} \quad o/w \end{cases}$$

$$y_{.t}^{i,j} = \begin{cases} y_{.t}^{i,j} + f_j, \quad if\ y_{.t}^{i,j} + f_j \leq R_j \\ R_j, \quad o/w \end{cases}$$

$$h = h + 1$$

(34)

Now, the disaggregate flows out of each cell i at any time t can be given by:

$$y_{s,t}^{i.} = \sum_{\tau=0}^{t-n_i} z_{\tau,t}^{l,i} \times y_{s,\tau}^{.en(l)} \quad \forall i \in C_l; l \in L; t \in \{n_i, \dots, T-1\}. \tag{35}$$

Since there is only one outgoing connector for all cells except the diverging type,

$$y_{s,t}^{i,j} = y_{s,t}^{i.}, \quad \forall i \in C - C_D; j \in \Gamma_i; s \in C_S; t \in \{n_i, \dots, T-1\}. \tag{36}$$

Note that this also applies to sink cells, which do not have any connectors and the outflows are zero. Further, it can be verified that the outflows from a diverging cell i are distributed as:

$$y_{s,t}^{i,j} = d_{s,t}^{i,j} \times y_{s,t}^{i.}, \quad \forall i \in C_D; j \in \Gamma_i; s \in C_S; t \in \{n_i, \dots, T-1\}. \tag{37}$$

Finally, the following proposition can be derived from eqs. (28) & (35).

Proposition 11:

$$y_{s,t}^{i.} = \begin{cases} \lim_{\varepsilon \to 0^+} \frac{y_{.t}^{i.} + \varepsilon}{y_{.A_t^{l,i}}^{.en(l)} + \varepsilon} \times y_{s,A_t^{l,i}}^{.en(l)} \quad if\ A_t^{l,i} = A_{t+1}^{l,i} \\ \lim_{\varepsilon \to 0^+} \frac{\tilde{y}_{.A_t^{l,i}}^{.en(l)} - \tilde{y}_{.t-1}^{i.}}{y_{.A_t^{l,i}}^{.en(l)} + \varepsilon} \times y_{s,A_t^{l,i}}^{.en(l)} + \sum_{\tau'=A_t^{l,i}+1}^{A_{t+1}^{l,i}-1} y_{s,\tau'}^{.en(l)} + \frac{\tilde{y}_{.t}^{i.} - \tilde{y}_{.A_t^{l,i}-1}^{.en(l)}}{y_{.A_t^{l,i}}^{.en(l)} + \varepsilon} \times y_{s,A_{t+1}^{l,i}}^{.en(l)} \quad o/w \end{cases} \quad \forall i \in C_l; l \in L; s \in C_S; t \in \{n_i, \dots, T-1\}. \tag{38}$$

Cost computations:

Several travel cost computation approaches have been proposed in earlier studies that range from the summation of travel costs of all the links on a path to its estimation using cumulative departures and cumulative arrivals at the origin and destination of a given path. However, since paths between each O-D pair are not enumerated in this study, the average travel costs entering each link at each time step are estimated here instead. In the following two subsections, recursive formulations are given to compute the average travel costs from the entry of each link and the marginal system costs with respect to the choice variables (departure time and turns at the diverge intersections), both of which include travel time and schedule delay components.

a) Average travel costs:

Without loss of generality, it is assumed here that all the flow capacities on a sink link are equal, and the storage capacities on all the non-sink links are equal. The storage capacity of a sink cell will, of course, be infinite. This guarantees that the sink links will always be under free-flow, as there is no possibility of congestion propagating from the downstream. This assumption is made only to make the representation of computations simpler, but the following methods should apply equally well for cases violating it. Now, the proportion of traffic that enters a given link l at time τ and reaches its destination s at time t is given by:

$$p_{s,\tau,t}^{l} = \begin{cases} 1, \quad if\ s = ex(l)\ and\ t = \tau + n_{ex(l)} - 1 \\ \sum_{\tau' \in \{\tau+1,\dots,T-1\}} z_{\tau,\tau'}^{l,ex(l)} \times p_{s,\tau',\tau}^{l'}, \quad if\ |X_l| = 1\ and\ l' \in X_l \\ \sum_{l' \in X_l} \sum_{\tau' \in \{\tau+1,\dots,T-1\}} z_{\tau,\tau'}^{l,ex(l)} \times d_{s,\tau'}^{ex(l),en(l')} \times p_{s,\tau',\tau}^{l'}, \quad if\ |X_l| > 1 \\ 0, \quad o/w \end{cases} \tag{39}$$

Using eq. (39), the average travel time for traffic entering link l at time τ and destined to s is given by:

$$TT_{s,\tau}^{l} = \sum_{t \in \{\tau,\dots,T-1\}} p_{s,\tau,t}^{l} \times (t-\tau) + \left(1 - \sum_{t \in \{\tau,\dots,T-1\}} p_{s,\tau,t}^{l}\right) \times (M + T - \tau) = (M + T - \tau) + \sum_{t \in \{\tau,\dots,T-1\}} p_{s,\tau,t}^{l} \times (t - M - T), \quad \forall\ l \in L; s \in C_S; \tau \in \{0, \dots, T-1\}. \tag{40}$$

M in the above equation is the penalty value assigned to vehicles that fail to reach their destinations before the end of simulation. Along with the average travel times, travels costs include average late arrival costs and early arrival costs, defined as follows:

$$e_{s,\tau}^{l} = \begin{cases} 0 \quad if\ \tau \geq t^{*s} \\ \sum_{t \in \{\tau,\dots,t^{*s}-1\}} p_{s,\tau,t}^{l} \times (t^{*s} - t) \quad o/w \end{cases}, \quad \forall l \in L; s \in C_S; \tau \in \{0, \dots, T-1\}. \tag{41}$$

$$f_{s,\tau}^{l} = \begin{cases} 0 \quad if\ s \in C_l\ and\ \tau \leq t^{*s} \\ \sum_{t \in \{\max\{t^{*s}+1,\tau\},\dots,T-1\}} p_{s,\tau,t}^{l} \times (t - t^{*s}) + \left(1 - \sum_{t \in \{\tau,\dots,T-1\}} p_{s,\tau,t}^{l}\right) \times (M + T - t^{*s}) \quad o/w \end{cases}, \quad \forall l \in L; s \in C_S; \tau \in \{0, \dots, T-1\}. \tag{42}$$

The average travel costs are given by appropriately weighting the above three components as follows:

$$TC_{s,\tau}^{l} = \alpha^{s} TT_{s,\tau}^{l} + \beta^{s} e_{s,\tau}^{l} + \gamma^{s} f_{s,\tau}^{l}, \quad \forall\ l \in L; s \in C_S; \tau \in \{0, \dots, T-1\}. \tag{43}$$

Proposition 12:

$$TT_{s,\tau}^{l} = \begin{cases} n_{ex(l)} - 1, \quad if\ s = ex(l)\ and\ \tau < T - n_{ex(l)} \\ \sum\limits_{\tau' \in \{\tau+1,\dots,T-1\}} z_{\tau,\tau'}^{l,ex(l)} \times \left(TT_{s,\tau'}^{l'} + \tau' - \tau\right) + \left(1 - \sum\limits_{\tau' \in \{\tau+1,\dots,T-1\}} z_{\tau,\tau'}^{l,ex(l)}\right) \times (M + T - \tau), \quad if\ |X_l| = 1\ and\ l' \in X_l \\ \sum\limits_{l' \in X_l} \sum\limits_{\tau' \in \{\tau+1,\dots,T-1\}} z_{\tau,\tau'}^{l,ex(l)} \times d_{s,\tau'}^{ex(l),en(l')} \times \left(TT_{s,\tau'}^{l'} + \tau' - \tau\right) + \left(1 - \sum\limits_{\tau' \in \{\tau+1,\dots,T-1\}} z_{\tau,\tau'}^{l,ex(l)}\right) \times (M + T - \tau), \quad if\ |X_l| > 1 \\ T - \tau, \quad o/w \end{cases}$$

$$e_{s,\tau}^{l} = \begin{cases} t^{*s} - \tau - n_{ex(l)} + 1, & if\ s = ex(l)\ and\ \tau + n_{ex(l)} < t^{*s} \\ \sum_{\tau' \in \{\tau+1,\dots,T-1\}} z_{\tau,\tau'}^{l,ex(l)} \times e_{s,\tau'}^{l'}, & if\ |\mathrm{X}_l| = 1\ and\ l' \in \mathrm{X}_l \\ \sum_{l' \in X_l} \sum_{\tau' \in \{\tau+1,\dots,T-1\}} z_{\tau,\tau'}^{l,ex(l)} \times d_{s,\tau'}^{ex(l),en(l')} \times e_{s,\tau'}^{l'}, & if\ |\mathrm{X}_l| > 1 \\ 0, & o/w \end{cases}$$

$$f_{s,\tau}^{l} = \begin{cases} \tau + n_{ex(l)} - 1 - t^{*s}, & if\ s = ex(l)\ and\ \tau + n_{ex(l)} > t^{*s} \\ \sum_{\tau' \in \{\tau+1,\dots,T-1\}} z_{\tau,\tau'}^{l,ex(l)} \times f_{s,\tau'}^{l'} + \left(1 - \sum_{\tau' \in \{\tau+1,\dots,T-1\}} z_{\tau,\tau'}^{l,ex(l)}\right) \times (M + T - t^{*s}), & if\ |\mathrm{X}_l| = 1\ and\ l' \in \mathrm{X}_l \\ \sum_{l' \in X_l} \sum_{\tau' \in \{\tau+1,\dots,T-1\}} z_{\tau,\tau'}^{l,ex(l)} \times d_{s,\tau'}^{ex(l),en(l')} \times f_{s,\tau'}^{l'} + \left(1 - \sum_{\tau' \in \{\tau+1,\dots,T-1\}} z_{\tau,\tau'}^{l,ex(l)}\right) \times (M + T - t^{*s}), & if\ |\mathrm{X}_l| > 1 \\ M + T - t^{*s}, & if\ ex(l) \in C_S\ and\ s \neq ex(l) \\ 0, & o/w \end{cases}$$

$$TC_{s,\tau}^{l} = \begin{cases} \alpha^s \times (n_{ex(l)} - 1) + I(\tau + n_{ex(l)} < t^{*s}) \times \beta^s \times (t^{*s} - \tau - n_{ex(l)} + 1) + I(\tau + n_{ex(l)} > t^{*s}) \times \gamma^s \times (\tau + n_{ex(l)} - 1 - t^{*s}), & if\ s = ex(l) \\ \gamma^s \times (M + T - t^{*s}) + \alpha^s \times (M + T - \tau) & if\ s \neq ex(l)\ and\ ex(l) \in C_S \\ \sum_{\tau' \in \{\tau+1,\dots,T-1\}} z_{\tau,\tau'}^{l,ex(l)} \times \left(TC_{s,\tau'}^{l'} + \alpha^s \times (\tau' - \tau)\right) + \left(1 - \sum_{\tau' \in \{\tau+1,\dots,T-1\}} z_{\tau,\tau'}^{l,ex(l)}\right) \times \left((\gamma^s + \alpha^s) \times (M + T)\right) - (\gamma^s \times t^{*s} + \alpha^s \times \tau), & if\ |\mathrm{X}_l| = 1\ and\ l' \in \mathrm{X}_l \\ \sum_{l' \in X_l} \sum_{\tau' \in \{\tau+1,\dots,T-1\}} z_{\tau,\tau'}^{l,ex(l)} \times d_{s,\tau'}^{ex(l),en(l')} \times \left(TC_{s,\tau'}^{l'} + \alpha^s \times (\tau' - \tau)\right) + \left(1 - \sum_{\tau' \in \{\tau+1,\dots,T-1\}} z_{\tau,\tau'}^{l,ex(l)}\right) \times \left((\gamma^s + \alpha^s) \times (M + T)\right) - (\gamma^s \times t^{*s} + \alpha^s \times \tau), & if\ |\mathrm{X}_l| > 1 \end{cases}$$

$$\forall\ l \in L; s \in C_S; \tau \in \{0, \dots, T-1\}. \tag{44}$$

Proof: All the recursive formulations can be verified using eqs. (39)-(43).

b) Total system cost (TSC) and marginal system costs (MCs):

While average travel costs are used for the calculation of the user equilibrium, marginal costs are used to determine the system optimum assignment. In this subsection, a formula for total system cost is given in terms of cell occupancies and marginal costs are computed with respect to the occupancies using an efficient, backpropagation procedure. Finally, marginal costs w.r.t. all the choice variables are determined, which are, unlink the travel costs, discontinuous. As will be seen in later sections, this should not pose a significant problem in their usage in determining the system optimum assignment.

Since it is not possible to derive a simple formula for TSC without introducing further cumbersome notation, only a sketch of the proof is provided here. But first, for the purpose of clarity, the vehicles are divided into three types: (a) Those that reached their respective destinations before their target times, (b) Those that reached their destinations after their target times but before the end of the simulation and (c) those that failed to reach their destinations. Now, the value of TSC can be given in terms of the cell occupancies as follows:

Proposition 13: $TSC = \sum_{t\in\{0,\dots,T_m-1\}} \sum_{\{(i,l)|i\in C_O\ \&\ i\in C_l\}} \sum_{s\in C_S} r_{s,t}^i \times D_s^i \times TC_{s,t}^l = \sum_{s\in C_S}\left(\alpha^s \times \sum_{i\in C-C_S} \sum_{\tau\in\{1,\dots,T\}} x_{s,\tau}^i\right) + \sum_{s\in C_S} \sum_{s'\neq s}\left(\alpha^s \times \sum_{\tau\in\{1,\dots,T\}} x_{s,\tau}^{s'}\right) + \sum_{s\in C_S}\left(\beta^s \times \left(-\sum_{\tau\le t^{*s}} x_{s,\tau}^s + t^{*s} \times x_{s,t^{*s}}^s\right) + \gamma^s \times \left(\sum_{\tau>t^{*s}} x_{s,\tau}^s - x_{s,T}^s \times (T - t^{*s})\right)\right) + (\gamma^s \times (M + T - t^{*s}) + \alpha^s \times M) \times \left(\sum_{i\in C-C_S} x_{s,T}^i + \sum_{s'\neq s} x_{s,T}^{s'}\right)$ (45)

The first term in eq. (45) gives the sum of all the occupancies of non-sink cells factored by their corresponding destination factors, and the second term gives the cost incurred during the simulation by the vehicles that got stuck in a wrong sink cell. These terms can be derived using the travel time equation in proposition 12 and all the flow equations, and their relation is easy to see by noting that the number of vehicles are conserved by the system. Similarly, the third term gives the late arrival and early arrival cost components for the vehicles that reached their destinations before the simulation time, which can be derived from the first conditionals of the early and late arrival cost formulas in proposition 12. And the final term gives the cost incurred by the vehicles failed to reach their destinations by the end of the simulation, which corresponds to the penalty imposed on the same.

Using the cell update equations (eqs. 1-12) and the flow computation equations (eqs. 13-38), the marginal costs of TSC w.r.t. each cell occupancy variable can be computed. Using a backpropagation technique to achieve this means beginning with the occupancy variables at the end of simulation ($x_{s,T}^i$) and providing recursive formulations corresponding to each type of cell.

First, the partial derivatives of TSC w.r.t. each occupancy variable can be given as follows:

$$\frac{\partial(TSC)}{\partial x_{s,\tau}^i} = \begin{cases} \alpha^s, & if\ i \in C - C_S\ or\ i \neq s\ and\ \tau < T \\ (\gamma^s \times (M + T - t^{*s}) + \alpha^s \times M), & if\ i \neq s\ and\ \tau = T \\ -\beta^s, & if\ i = s\ and\ \tau < t^{*s} \\ \beta^s \times (t^{*s} - 1), & if\ i = s\ and\ \tau = t^{*s} \\ \gamma^s, & if\ i = s\ and\ t^{*s} < \tau < T \\ \gamma^s \times (1 - T + t^{*s}), & if\ i = s\ and\ \tau = T \end{cases} \tag{46}$$

The marginal costs w.r.t. the occupancies of each ordinary cell (C_O) before the end of the simulation ($\tau < T$)are given by:

$$\frac{d(TSC)}{dx_{s,\tau}^i} = \alpha^s + \frac{d(TSC)}{dx_{s,\tau+1}^i} + I\left(x_\tau^i = y_{\cdot\tau}^{i\cdot}\right) \times \left(\frac{d(TSC)}{dx_{s,\tau+1}^j} - \frac{d(TSC)}{dx_{s,\tau+1}^i}\right) + I\left(y_{\cdot\tau}^{\cdot i} = \delta^i \times \left(N^i - x_\tau^i\right)\right) \times \left(-\delta^i \times \sum_{s\in C_S} g_{s,\tau+1}^j \times \left(\frac{d(TSC)}{dx_{s,\tau+1}^i} - \frac{d(TSC)}{dx_{s,\tau+1}^k}\right)\right) \tag{47}$$

where $g_{s,\tau}^i = \frac{y_{s,A_{s,\tau}^i}^{en(l)}}{y_{\cdot A_{s,\tau}^i}^{en(l)}}$.

Note that the third component in the above equation cannot be active when $y^{en(l)}_{\cdot A^{i}_{s,\tau+1}} = 0$ because that indicates a free-flow situation.

Unlike the midsection flows, flows at intersections are calculated using algorithms, which makes the calculation of marginal costs w.r.t. all the relevant occupancies less straightforward. However, formulas for the same can still be derived by considering the possible cases exhaustively. Thus, the marginal costs at a merging intersection can be given as follows:

$$\frac{d(TSC)}{dx^{i}_{s,\tau}} = \alpha^{s} + \frac{d(TSC)}{dx^{i}_{s,\tau+1}} + I\left(x^{i}_{\tau} = y^{i\cdot}_{\cdot\tau}\right) \times \left(\frac{d(TSC)}{dx^{j}_{s,\tau+1}} - \frac{d(TSC)}{dx^{i}_{s,\tau+1}}\right) - I\left(y^{\cdot i}_{\cdot\tau} = \delta^{i} \times \left(N^{i} - x^{i}_{\tau}\right)\right) \times \delta^{i} \times \sum_{k\in V} \frac{Q_k}{\sum_{k'\in V} Q_{k'}} \times \sum_{s\in C_S} g^{j}_{s,\tau+1} \times \left(\frac{d(TSC)}{dx^{i}_{s,\tau+1}} - \frac{d(TSC)}{dx^{k}_{s,\tau+1}}\right) \tag{48}$$

where $V = \left\{k \middle| k \in \Gamma_i^{-1}\ and\ y^{k,i}_{\cdot\tau} \neq \min\{x^{k}_{\tau}, Q_k\}\right\}$.

$$\frac{d(TSC)}{dx^{k}_{s,\tau}} = \alpha^{s} + \frac{d(TSC)}{dx^{k}_{s,\tau+1}} + I\left(x^{k}_{\tau} = y^{i\cdot}_{\cdot\tau}\right) \times \left[\left(\frac{d(TSC)}{dx^{i}_{s,\tau+1}} - \frac{d(TSC)}{dx^{k}_{s,\tau+1}}\right) + I\left(y^{\cdot i}_{\cdot\tau} = \delta^{i} \times \left(N^{i} - x^{i}_{\tau}\right)\right) \times \sum_{k\in V} \frac{Q_k}{\sum_{k'\in V} Q_{k'}} \times \sum_{s\in C_S} g^{j}_{s,\tau+1} \times \left(\frac{d(TSC)}{dx^{i}_{s,\tau+1}} - \frac{d(TSC)}{dx^{k}_{s,\tau+1}}\right)\right] + I\left(y^{\cdot i}_{\cdot\tau} = \delta^{i} \times \left(N^{i} - x^{i}_{\tau}\right)\right) \times \left(-\delta^{i} \times \sum_{s\in C_S} g^{j}_{s,\tau+1} \times \left(\frac{d(TSC)}{dx^{i}_{s,\tau+1}} - \frac{d(TSC)}{dx^{k}_{s,\tau+1}}\right)\right) \tag{49}$$

$\forall\ i \in C_M; k \in \Gamma_i^{-1}; s \in C_S; \tau \in \{0, \dots, T-1\}$.

Similarly, the marginal costs at a diverging intersection can be calculated as follows:

$$\frac{d(TSC)}{dx^{i}_{s,\tau}} = \alpha^{s} + \frac{d(TSC)}{dx^{i}_{s,\tau+1}} + I\left(x^{i}_{\tau} = y^{i\cdot}_{\cdot\tau}\right) \times \sum_{j\in\Gamma_i} d^{i,j}_{s,\tau} \times \left(\frac{d(TSC)}{dx^{j}_{s,\tau+1}} - \frac{d(TSC)}{dx^{i}_{s,\tau+1}}\right) + I\left(y^{\cdot i}_{\cdot\tau} = \delta^{i} \times \left(N^{i} - x^{i}_{\tau}\right)\right) \times \left(-\delta^{i} \times \sum_{s\in C_S} g^{j}_{s,\tau+1} \times \left(\frac{d(TSC)}{dx^{i}_{s,\tau+1}} - \frac{d(TSC)}{dx^{k}_{s,\tau+1}}\right)\right) \tag{50}$$

$$\frac{d(TSC)}{dx^{j}_{s,\tau}} = \alpha^{s} + \frac{d(TSC)}{dx^{j}_{s,\tau+1}} + I\left(x^{i}_{\tau} = y^{i\cdot}_{\cdot\tau}\right) \times \left(\frac{d(TSC)}{dx^{j}_{s,\tau+1}} - \frac{d(TSC)}{dx^{i}_{s,\tau+1}}\right) + I\left(y^{i,j}_{\cdot\tau} = \delta^{j} \times \left(N^{j} - x^{j}_{\tau}\right)\right) \times \left(-\delta^{j} \times \sum_{s\in C_S} g^{i}_{s,\tau+1} \times \sum_{j'\in\Gamma_i} d^{i,j'}_{s,\tau} \times \left(\frac{d(TSC)}{dx^{j'}_{s,\tau+1}} - \frac{d(TSC)}{dx^{i}_{s,\tau+1}}\right)\right) \tag{51}$$

$\forall\ i \in C_D; j \in \Gamma_i; s \in C_S; \tau \in \{0, \dots, T-1\}$.

And finally, the marginal costs w.r.t. the actual choice variables are given by:

$$\frac{\partial(TSC)}{\partial d^{i,j}_{s,\tau}} = y^{i\cdot}_{s,\tau} \times \left(\frac{d(TSC)}{dx^{j}_{s,\tau}} - \frac{d(TSC)}{dx^{i}_{s,\tau}}\right), \quad \forall\ i \in C_D; j \in \Gamma_i; s \in C_S; \tau \in \{0, \dots, T-1\}. \tag{52}$$

$$\frac{\partial(TSC)}{\partial r^{i}_{s,\tau}} = \begin{cases} D^{i}_{s} \times \frac{d(TSC)}{dx^{i}_{s,\tau}}, & \tau \leq T_m \\ 0, & o/w \end{cases}, \quad \forall\ i \in C_O; s \in C_S; \tau \in \{0, \dots, T-1\}. \tag{53}$$

Problem formulations:

a) User equilibrium dynamic traffic assignment:

Multiple studies have previously formulated the UE-DTA model with an embedded path-based CTM as a set of complementarity conditions to prove solution existence and other important properties (Han et al., 2011; Ukkusuri et al., 2012; Doan et al., 2015). The same is accomplished in this section with the proposed node-based CTM by using analogous steps to those in the previous studies. First, the travel cost equation will be rewritten in terms of the new auxiliary variables introduced below:

$$v_{s,\tau,t}^{l} = max\{0, \tau - \sum_{t'=0}^{t-1} Z_{s,\tau,t'}^{l.}\}, \quad \forall l \in L; s \in C_S; \tau, t \in \{0, \dots, T-1\}. \tag{54}$$

This implies

$$TC_{s,0}^{l} = \sum_{t'=1}^{T-1}\left(v_{s,0,t'}^{l} - v_{s,0,t'+1}^{l}\right) \times \left(\alpha^{s} \times t' + \sum_{l' \in \mathrm{X}_l} d_{s,t'}^{ex(l),en(l')} \times TC_{s,t'}^{l'}\right) + \left(1 - v_{s,0,1}^{l} + v_{s,0,T}^{l}\right) \times (\gamma^{s} \times (M + T - t^{*s}) + \alpha^{s} \times T), \quad \forall l \in L - L_S; s \in C_S. \tag{55}$$

$$TC_{s,\tau}^{l} = \sum_{t'=\tau}^{T-1}\left(v_{s,\tau,t'}^{l} - v_{s,\tau,t'+1}^{l} + v_{s,\tau-1,t'+1}^{l} - v_{s,\tau-1,t'}^{l}\right) \times \left(t' - \tau + \sum_{l' \in \mathrm{X}_l} d_{s,t'}^{ex(l),en(l')} \times TC_{s,t'}^{l'}\right) + \left(1 - v_{s,\tau,\tau}^{l} + v_{s,\tau,T}^{l} - v_{s,\tau-1,T}^{l} + v_{s,\tau-1,\tau}^{l}\right) \times \left(\gamma^{s} \times (M + T - t^{*s}) + \alpha^{s} \times (M + T - \tau)\right), \quad \forall\, l \in L - L_S; s \in C_S; \tau \in \{1, \dots, T-1\}. \tag{56}$$

Now, the max operator in eq. can be replaced by the complementarity conditions:

$$0 \le v_{s,\tau,t}^{l} \perp v_{s,\tau,t}^{l} - \left(\tau - \sum_{t'=0}^{t-1} Z_{s,\tau,t'}^{l.}\right) \ge 0, \quad \forall l \in L; s \in C_S; t \in \{0, \dots, T-1\}. \tag{57}$$

Next, for a DUE solution with the above model to be valid, it must satisfy conditions similar to Wardrop's first principle that correspond both to departure time choice variables for each O-D pair, and turning choice variables at each diverging intersection. When a given variable has a positive value for a traffic destined to s, the average travel cost from the entry of the link (a source link, in the first case; and an outgoing link from a diverging intersection, in the second) corresponding to that variable must be minimal. These conditions can be expressed in the complementarity form as follows:

$$0 \le r_{s,t}^{en(l)} \perp TC_{s,t}^{l} - C_{s,t}^{l*} \ge 0, \quad \forall l \in L_R; s \in C_S; t \in \{0, \dots, T-1\}. \tag{58}$$

$$0 \le d_{s,t}^{ex(l),en(l')} \perp TC_{s,t}^{l'} - C_{s,t}^{l*} \ge 0, \quad \forall l \in L; l' \in \mathrm{X}_l; s \in C_S; t \in \{0, \dots, T-1\}. \tag{59}$$

Similarly, the demand satisfaction conditions are given in complementarity form as follows:

$$0 \le C_{s,t}^{l*} \perp \sum_{t=0}^{T-1} r_{s,t}^{en(l)} - 1 \ge 0, \quad \forall l \in L_R; s \in C_S; t \in \{0, \dots, T-1\}. \tag{60}$$

$$0 \le C_{s,t}^{l*} \perp \sum_{l' \in \mathrm{X}_l} d_{s,t}^{ex(l),en(l')} - 1 \ge 0, \quad \forall l \in L; l' \in \mathrm{X}_l; s \in C_S; t \in \{0, \dots, T-1\}. \tag{61}$$

It will be shown later that, in the solution of the given formulation, the right-hand sides of the above two conditions hold as equalities, as expected from the nature of those variables. This completes the complementarity formulation, which includes eqs. (1)-(38).

b) System optimum dynamic traffic assignment:

The dynamic system optimum formulation can be given as an optimization problem with the total system cost (TSC) given by eq. (45) as the objective function to be minimized, the CTM formulation given by eqs. (1)-(38) as the constraints, and with the departure time choices ($r_{s,t}^{en(l)}$) and turning choices ($d_{s,t}^{i,j}$) as the decision variables. Despite the node-based framework of the described CTM, this DSO model is very similar to the path-based one in Doan & Ukkusuri (2015) and several of the nice properties of this earlier model, including the solution existence, can be shown to extend to the present formulation. Firstly, since all the flow functions in the presented CTM are continuous, TSC must also be a continuous function. And since all the decision variables can be divided into independent sets of proportion-like variables, the feasible region is convex and bounded. Furthermore, the value of the objective function (TSC) is bounded below by zero. Thus, the solution for the proposed formulation always exists. It can similarly be shown that the marginal costs (eqs. 52 & 53) play the same role in the present DSO problem as a few travel costs do in the DUE problem, using the following relaxed lagrangian function of the optimization problem:

$$L = TSC + \sum_{i\in C_O}\sum_{s\in C_S} l_s^i \times \left(D_s^i - \sum_{t\in\{0,\dots,T_m\}} r_{s,t}^i\right) + \sum_{i\in C_D}\sum_{t\in\{0,\dots,T-1\}} m_{s,t}^i \times \left(1 - \sum_{j\in\Gamma_i} d_{s,t}^{i,j}\right) \quad (62)$$

Thus, the first-order conditions of the node-based DSO problem can be given by:

$$r_{s,t}^{*i} \times \left(\frac{\partial(TSC)}{\partial r_{s,t}^i} - l_s^i\right) = 0;\ \frac{\partial(TSC)}{\partial r_{s,t}^i} - l_s^i \geq 0;\ D_s^i - \sum_{t\in\{0,\dots,T_m\}} r_{s,t}^i = 0;\ r_{s,t}^i \geq 0,\quad \forall\, i \in C_O; s \in C_S; t \in \{0,\dots,T-1\}. \quad (63)$$

$$d_{s,t}^{*i,j} \times \left(\frac{\partial(TSC)}{\partial d_{s,t}^{i,j}} - m_{s,t}^i\right) = 0;\ \frac{\partial(TSC)}{\partial d_{s,t}^{i,j}} - m_{s,t}^i \geq 0;\ 1 - \sum_{j\in\Gamma_i} d_{s,t}^{i,j} = 0;\ d_{s,t}^{i,j} \geq 0,\quad \forall\, i \in C_D;\ j \in \Gamma_i; s \in C_S; t \in \{0,\dots,T-1\}. \quad (64)$$

Both types of equation sets above correspond to the Wardrop's first principle-based conditions of the DUE problem (eqs. 58 & 60, and eqs. 59 & 61), except that the marginal costs are used here instead of the average travel costs. This similarity allows the formulation of the DSO problem as a complementarity problem and the usage of the same kind of algorithms for both the problems. Further details in this regard are omitted in the present study, but it involves duplication of much of what is presented in the previous subsection, after redefining discontinuous marginal costs as set-valued maps.

The complementarity formulations of both UE and SO models can be transformed into equivalent variational inequality (VI) and generalized variational inequality (GVI) problems, respectively. These equivalencies can be proven almost exactly as for the problems in Ukkusuri et al. (2012) and, therefore, we proceed to the solution algorithm for the proposed models.

Solution algorithm:

Ukkusuri et al. (2012) developed an efficient solution algorithm for $VI(K,F)$ based on a classical approach to solve VI problems called projection method. In this method, for a given initial solution x^0, a sequence of points can be computed as follows:

$$x^{k+1} = \prod_K \left(x^k - F(x^k)\right), \forall k = 1,2,\dots \tag{65}$$

where $\prod_K(x)$ is the projection of x on K, i.e., $\prod_K(x) = arg\,min_{z\in K}\|z - x\|^2$. Under certain conditions, which include the monotonicity of F, it can be shown that $lim_{l\to\infty} x^l = x^*$, where x^* is a solution of $VI(K,F)$. The convergence also happens when F is non-monotonic but K is compact. The propositions establishing the convergence of the projection algorithm for both formulations are restated here for completion, and their proofs follow from the fact that any sequence in a compact set has a convergent subsequence.

Proposition 14: Let $\boldsymbol{r}^0 \in \boldsymbol{\Omega}$ and $\boldsymbol{r}^{l+1} = \prod_{\boldsymbol{\Omega}}(\boldsymbol{r}^l - C^a(\boldsymbol{r}^l)), \forall l = 1,2,\dots$. Then there exists a subsequence $\{\boldsymbol{r}^{l_k}\}_{k=1}^{\infty}$ such that $lim_{k\to\infty} \boldsymbol{r}^l = \boldsymbol{r}^*$, which is a solution of $VI(\Omega, C^a)$. Moreover, any limiting points of $\{\boldsymbol{r}^{l_k}\}_{k=1}^{\infty}$ is a solution of $VI(\Omega, C^a)$.

Proposition 15: For a VI/GVI problem equivalent to either of the proposed complementarity formulations, let $\boldsymbol{r}^l$ be generated as described in proposition 14. The following statements hold for such a sequence:

a) There exists a convergent subsequence of $\{\boldsymbol{r}^l\}_{l=0}^{\infty}$.

b) For any convergent subsequence of $\{\boldsymbol{r}^l\}_{l=0}^{\infty}$, the limiting point $\boldsymbol{r}^*$ is a solution of the complementarity formulation.

Now, with all the necessary properties of the formulation established, the same projection algorithm used in Ukkusuri et al. (2012) can be used for the present model:

1) Set $k = 0$. Initialize the departure time choice and turning choices with some feasible values $\boldsymbol{r}^0, \boldsymbol{d}^0$.

2) Run the simulation and compute $CTM(\boldsymbol{r}^k, \boldsymbol{d}^k), C(\boldsymbol{r}^k, \boldsymbol{d}^k)$.

3) Solve the quadratic program: $\boldsymbol{z}^* = arg\,min \left\| z - \left((\boldsymbol{r}^k, \boldsymbol{d}^k) - \lambda C(\boldsymbol{r}^k, \boldsymbol{d}^k)\right)\right\|^2$.

4) If $\|z - \boldsymbol{r}^k\| < \epsilon$, terminate the algorithm with $\boldsymbol{r}^* = \boldsymbol{z}^*$. Otherwise, $\boldsymbol{r}^{k+1} = \boldsymbol{z}^*$, $k = k + 1$ and go to step 1.

The costs $C(\boldsymbol{r}^k, \boldsymbol{d}^k)$ used in the above algorithm are average travel costs in the case of the UE problem and marginal costs divided by the average demand per O-D pair in the case of the SO problem. The scaling of the marginal costs could be avoided by choosing an appropriate learning rate but is made to keep all the costs in the later experiments within similar ranges to facilitate their comparisons. Also, note that λ is the learning rate parameter whose choice affects the speed and accuracy of the solution. A detailed discussion of this issue can be found in the numerical results section. Note that the proposed models involve multiple sets of proportion variables in terms of which both the objective function and the constraints are separable in the algorithm. Therefore, it may be more efficient in terms of both memory and time to solve the quadratic program in each iteration separately for each set of proportion variables.

Numerical results:

In this section, the proposed models and algorithms are applied to two standard test networks: the first one (fig. 3a), originally used in Ziliaskopoulos (2000), has 10 cells, two diverging sections and a single O-D pair (1-10), and the second one (fig. 3b), originally given in Nguyen & Dupuis (1984), has 57 cells, eight diverging intersections and four O-D pairs (1-48; 1-57; 14-48; 14-57). Unlike in the previous studies, no predefined paths are used in the experiments. The cell length in both the cases is 0.5 miles, and the free-flow speed and congestion wave factor of the vehicle type are 30 mph and 0.8, respectively. All the roads have three lanes, and their jam density and flow capacity are 160 vehicles/mile/lane and 24 vehicles/minute/lane, respectively. For simplicity, the same travel cost factors are used for all sinks (α_s=1; β_s=0.5; γ_s=2). For Ziliaskopoulos' network, the target time, maximum departure time and maximum time horizon are 110, 160 and 170, respectively; whereas the same for the Nguyen-Dupuis' network are 60, 80 and 132, respectively.

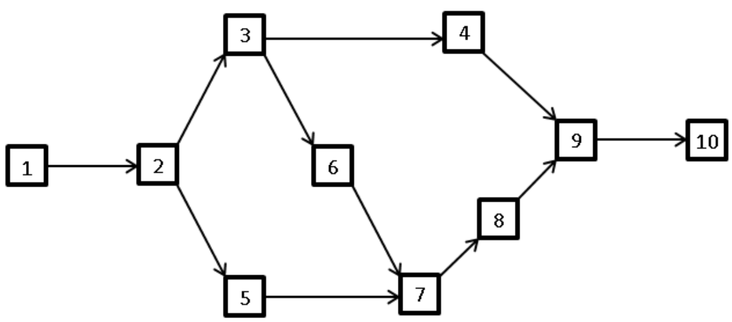

(a)

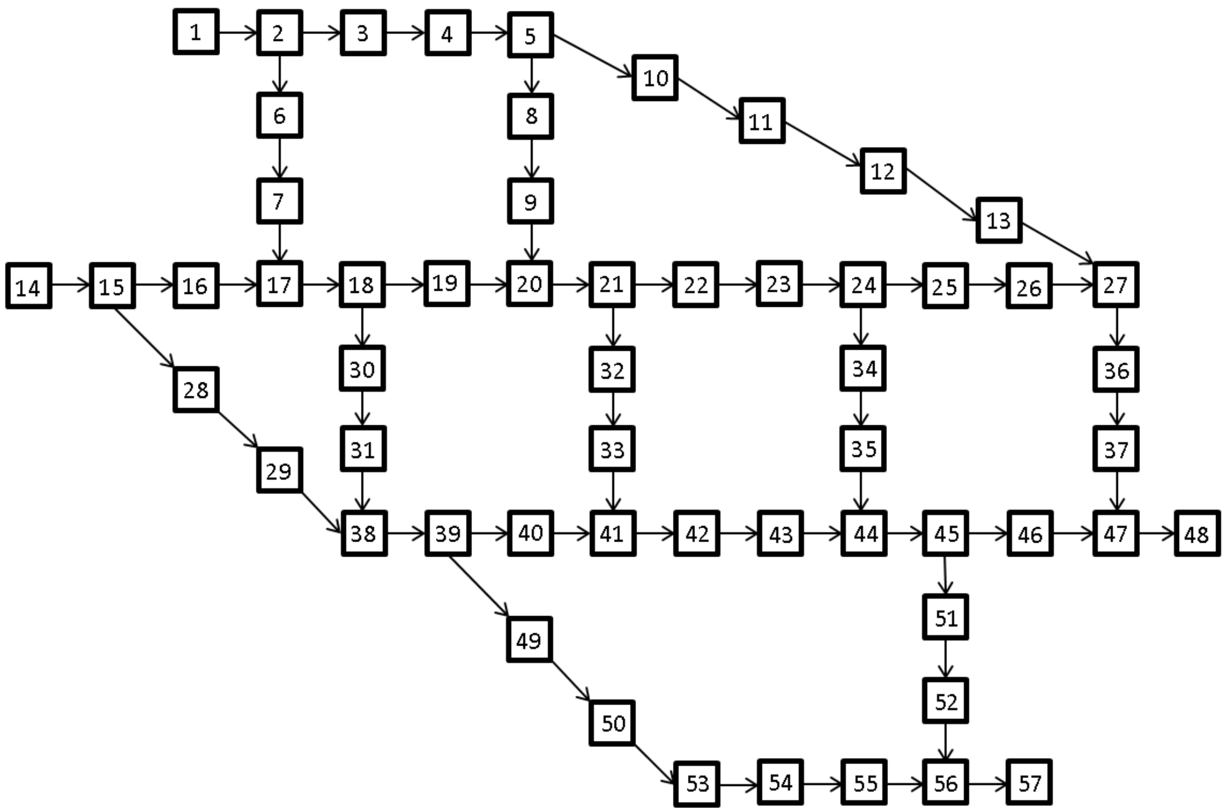

(b)

Figure 3: Test networks: (a) Ziliaskopoulos' network, (b) Nguyen-Dupuis' network

The experiments were conducted by varying total demands between each O-D pair (450, 900, 1350, 1800) and learning rates in the projection algorithm (0.01, 0.001, 0.0001). The convergence of the algorithms is observed using the following measures:

a) The norm of the difference between two consecutive departure time choice variable solutions.
b) The norm of the difference between two consecutive turning choice variable solutions, averaged across all the diverging intersections.
c) A relative gap measure corresponding to the departure time choice variables given by:

$$g_1 = \frac{1}{|C_O| \times |C_S|} \times \sum_{\{i,l|i \in C_O \,\&\, en(l)=i\}} \sum_{s \in C_S} \frac{\sum_{t \in \{0,\dots,T_m-1\}} \left(r_{s,t}^i \times C_{s,t}^l - C_s^{*l} \right)}{C_s^{*l} + \mu},$$

where $C_s^{*l} = \min_{t \in \{0,\dots,T_m-1\}} C_{s,t}^l$.

d) A relative gap measure corresponding to the turning choice variables given by:

$$g_2 = \frac{1}{|C_D|} \sum_{i \in C_D} \frac{\sum_{s \in C_S} \sum_{t \in \{0,\dots,T-1\}} \sum_{j \in \Gamma_i} \left(d_{s,t}^{i,j} \times C_{s,t}^{i,j} - C_{s,t}^{*i} \right)}{\sum_{s \in C_S} \sum_{t \in \{0,\dots,T-1\}} C_{s,t}^{*i} + \mu},$$

where $C_{s,t}^{*i} = \min_{j \in \Gamma_i} C_{s,t}^{i,j}$.

The relevant average travel costs ($TC^{l}_{s,t}$) and scaled marginal costs ($\frac{\partial(TSC)}{\partial r^{i}_{s,t}}/D_{mean}$ & $\frac{\partial(TSC)}{\partial d^{i,j}_{s,t}}/D_{mean}$) take the place of the above cost variables for the UE & SO problems, respectively. Since the latter has a clearly defined and efficiently computable objective function, its value could be used as an additional performance indicator. But to make the comparison across different demand levels, the average travel cost is used here instead.

a) Initialization of the choice variables:

The following strategy is chosen for the initialization of the variables after conducting several experiments: all the traffic between each O-D pair is departed at the maximum departure time, and all the turning choices at the diverging intersections are made towards the link with the least free-flow travel cost. As will be observed later, the turning choices remain as initialized for both UE and SO problems at different demand levels. And the high travel costs at the maximum departure times lead to faster convergence to the desired solution.

b) Results of the experiments:

Note that the axes of all the subplots in the figures below are clipped for improving the interpretability of the plots. In almost all the cases, this has only affected the visibility of the values in the initial iterations.

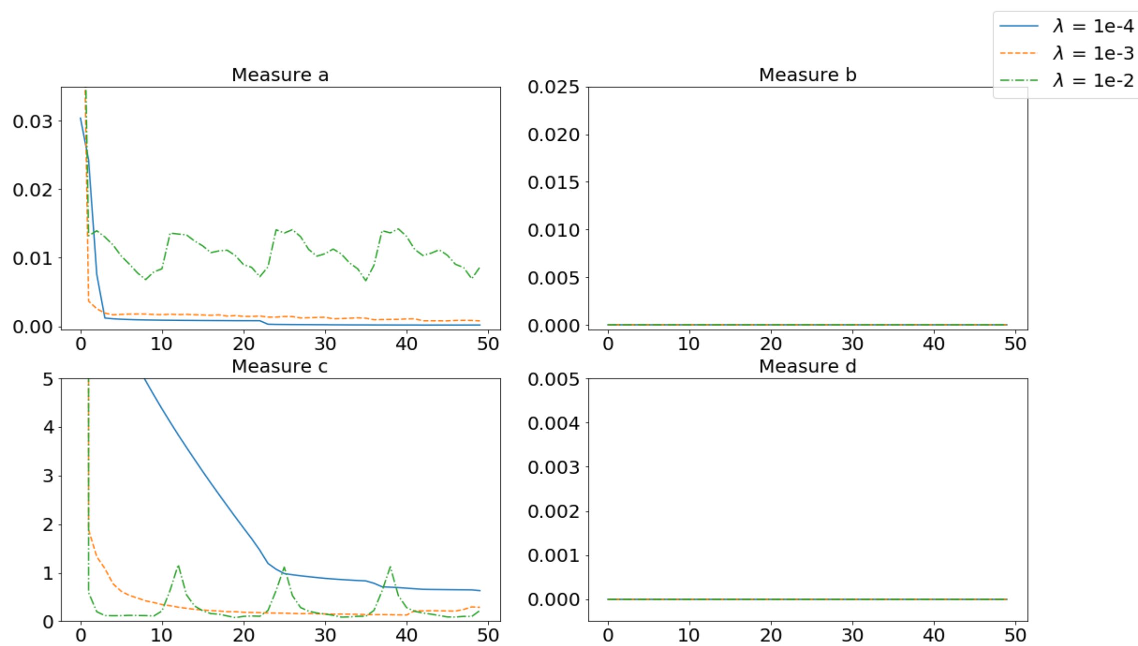

(a)

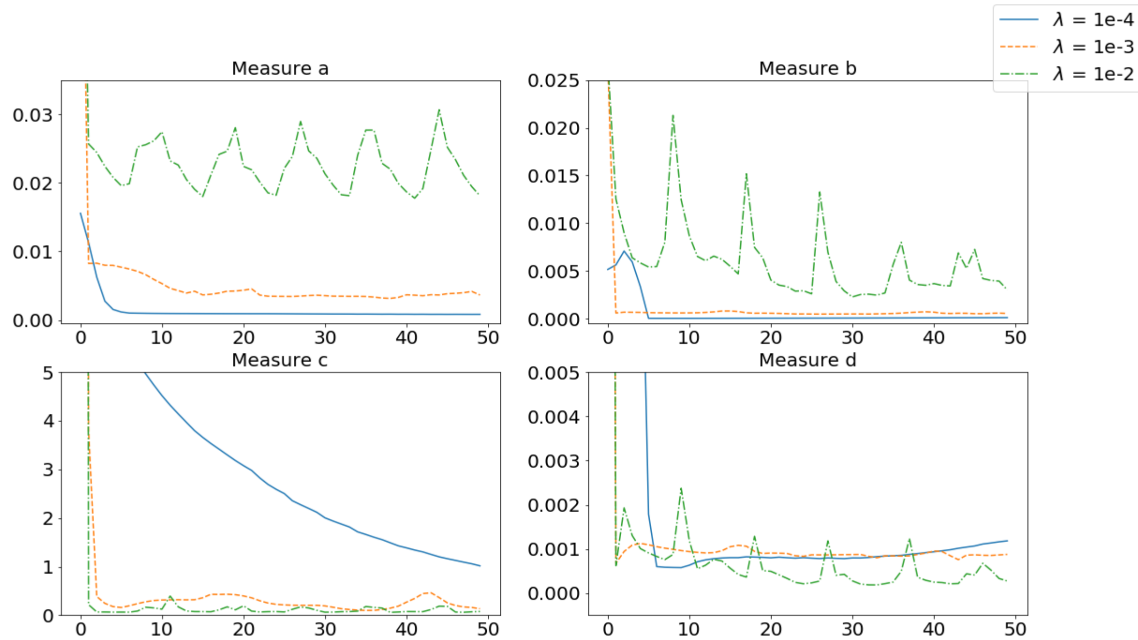

(b)

Figure 4: Values of the convergence measures for the first 50 iterations of the user equilibrium algorithm at a demand per O-D pair of 1800 vehicles with (a) Ziliaskopoulos' network; (b) Nguyen-Dupuis' network. All the x-axes of the subplots indicate iteration number and y-axes indicate measure value.

All the results in figure 4 conform to the common observation made regarding the convergence of optimization algorithms with a learning rate parameter: larger learning rate gives a faster convergence to a suboptimal solution, whereas smaller learning rate may lead to a better solution, but with slow convergence. Firstly, note that all the values for measures b and d in the case of Ziliaskopoulos network are zero, which means all the turning choices in that case remain as they were at the beginning of the algorithm. Also, notice that the value of measure c in both cases is significantly greater for the learning rate of 1e-4. This indicates that despite the availability of a better departure time, the demand is unable to shift to it because of the small learning rate. On the other hand, the values for the learning rate of 1e-2 display periodicity in almost all the cases. Here, the traffic seems to be shifting too rapidly, resulting in a sharp increase in the travel costs of the new choice and a sharp decrease in the same of the starting choice. This leads to the traffic oscillating between two different portions of the choices as the iterations continue. Overall, the learning rate 1e-3 seems to largely avoid both the problems, arriving at a nearly optimal solution quickly and avoiding rapid shifting of the traffic to new choices.

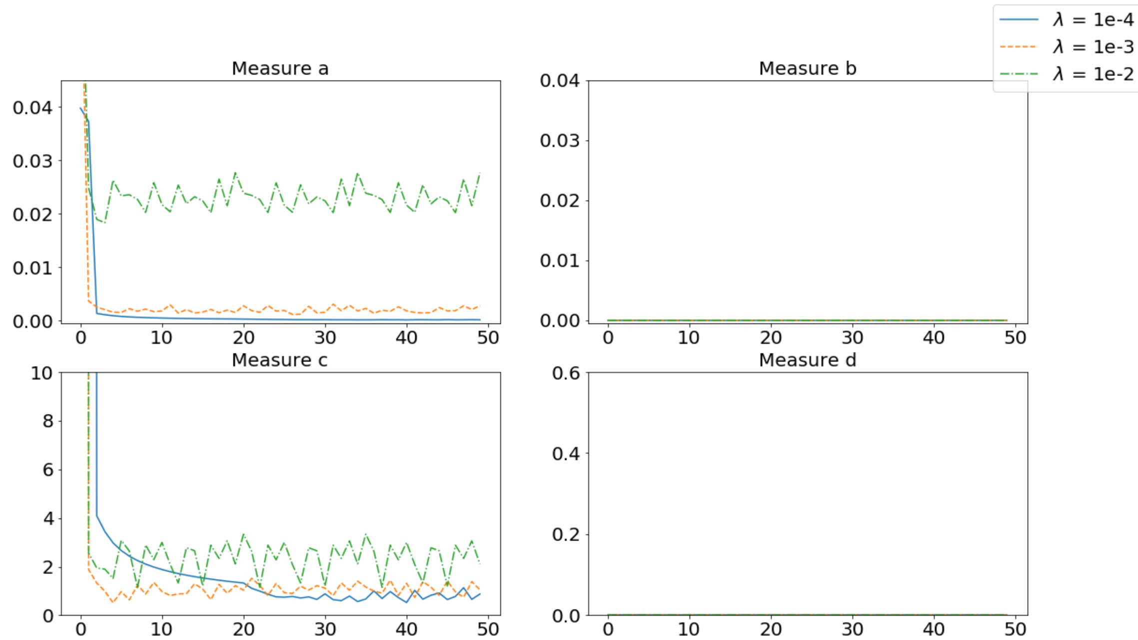

(a)

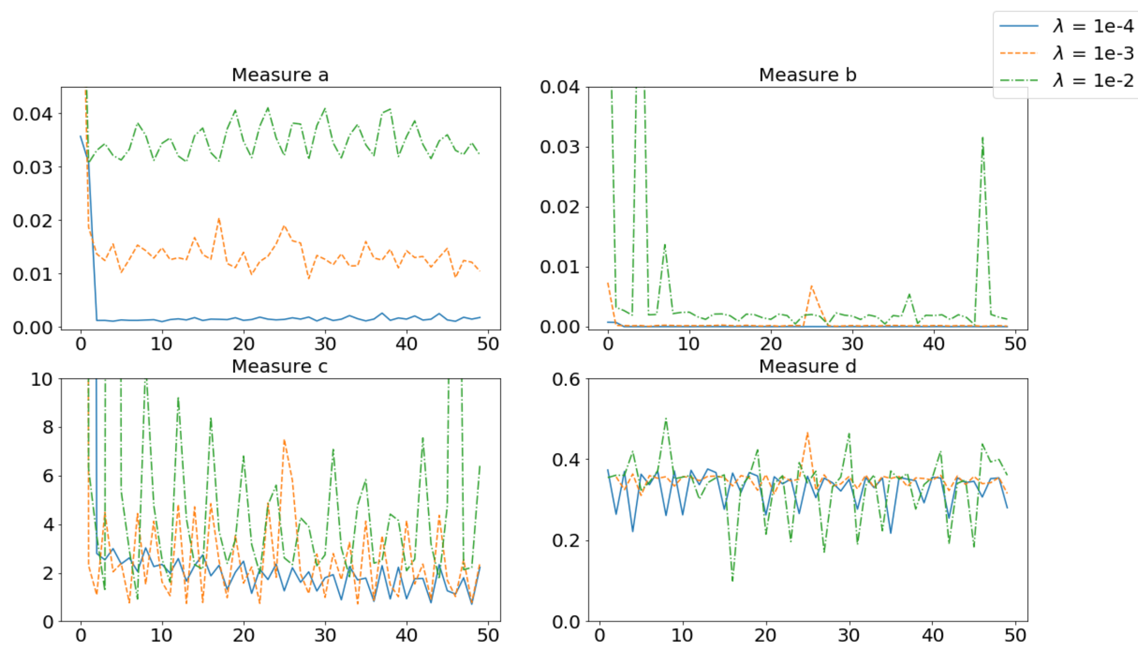

(b)

Figure 5: Values of the convergence measures for the first 50 iterations of the system optimum algorithm at a demand per O-D pair of 1800 vehicles with (a) Ziliaskopoulos' network; (b)

Nguyen-Dupuis' network. All the x-axes of the subplots indicate iteration number and y-axes indicate measure value.

The results shown in figure 5 are similar to those in figure 4 in two ways: the turning choices do not change in any experiment for Ziliaskopoulos' network, and the larger learning rates lead to suboptimal solutions and the start fluctuating around it as the iterations continue. However, any of the measures, especially the gap measures, seem highly sensitive to the changes in successive iterations and they do not display the same level of convergence as with the user equilibrium algorithm. But their volatility is lower for smaller learning rates. As seen in figure 6, this does not result in a failure of the algorithm to obtain good solutions for small enough learning rates.

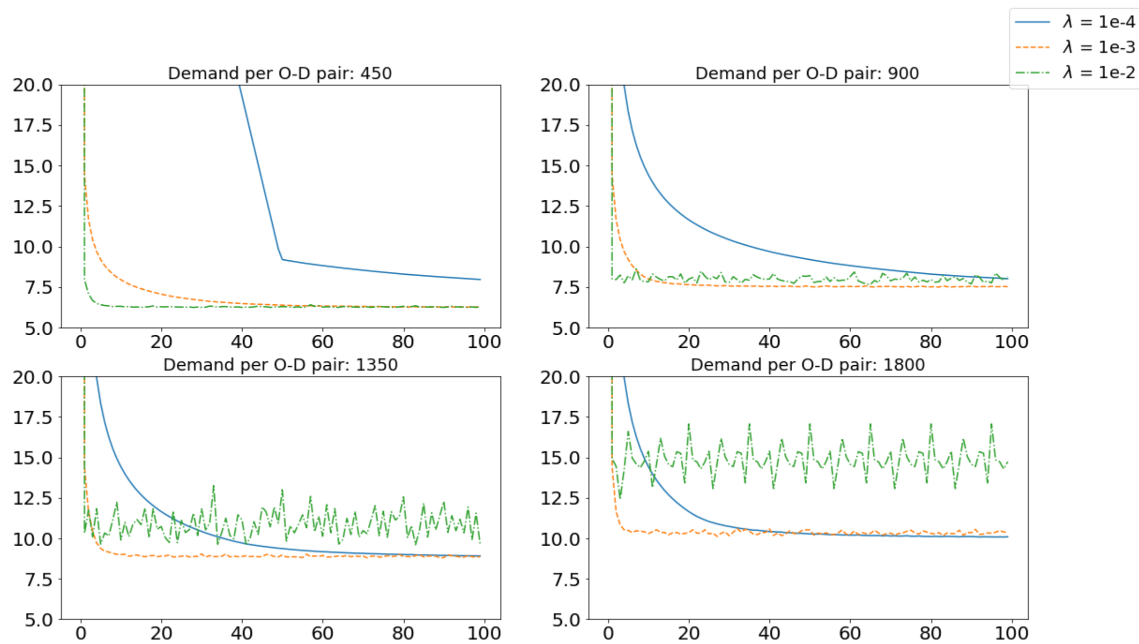

(a)

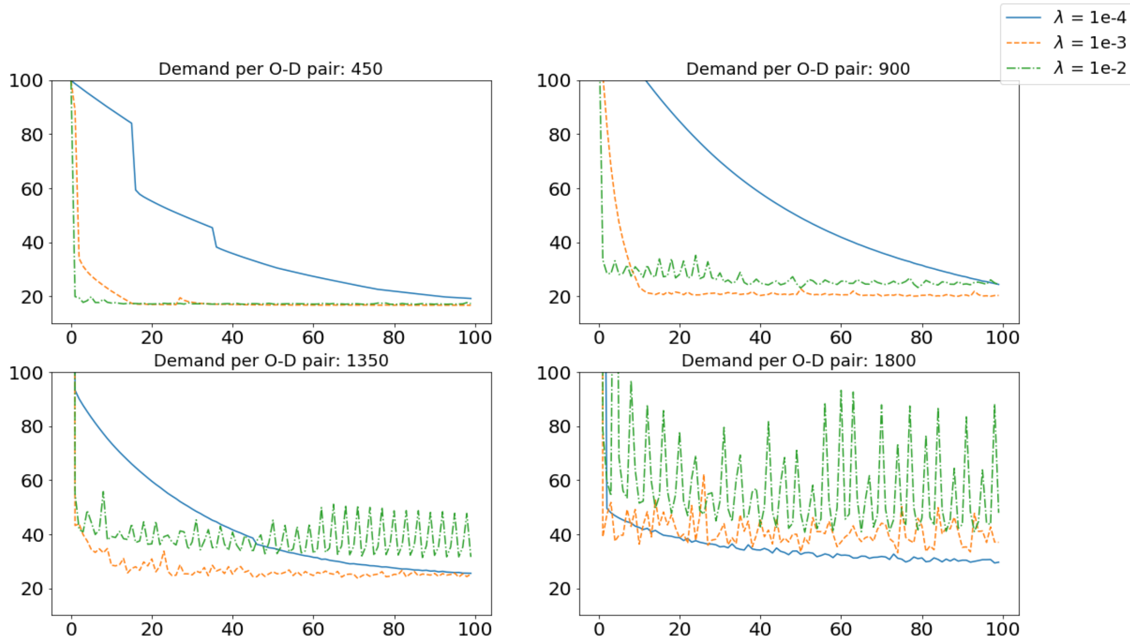

(b)

Figure 6: Average travel costs for the first 100 iterations of the system optimum algorithm at different demand levels for (a) Ziliaskopoulos' network; (b) Nguyen-Dupuis' network. All the x-axes of the subplots indicate iteration number and y-axes indicate measure value.

The effect of learning rate on average travel costs is again clear in figure 6: smaller learning rates eventually give better solutions but significantly more number of iterations. Further, the optimal value of learning rate seems to decrease as the demand per O-D pair increases. There is also a phenomenon of sharp drops and rises in the average cost value, which is especially pronounced for smaller demand levels (top-left subplot in figure 6b). Figure 7 shows the correlation between such sharp changes in the average cost and the spikes observed in measure c for Nguyen-Dupuis' network at a demand per O-D pair of 450 vehicles and a learning rate of 1e-4.

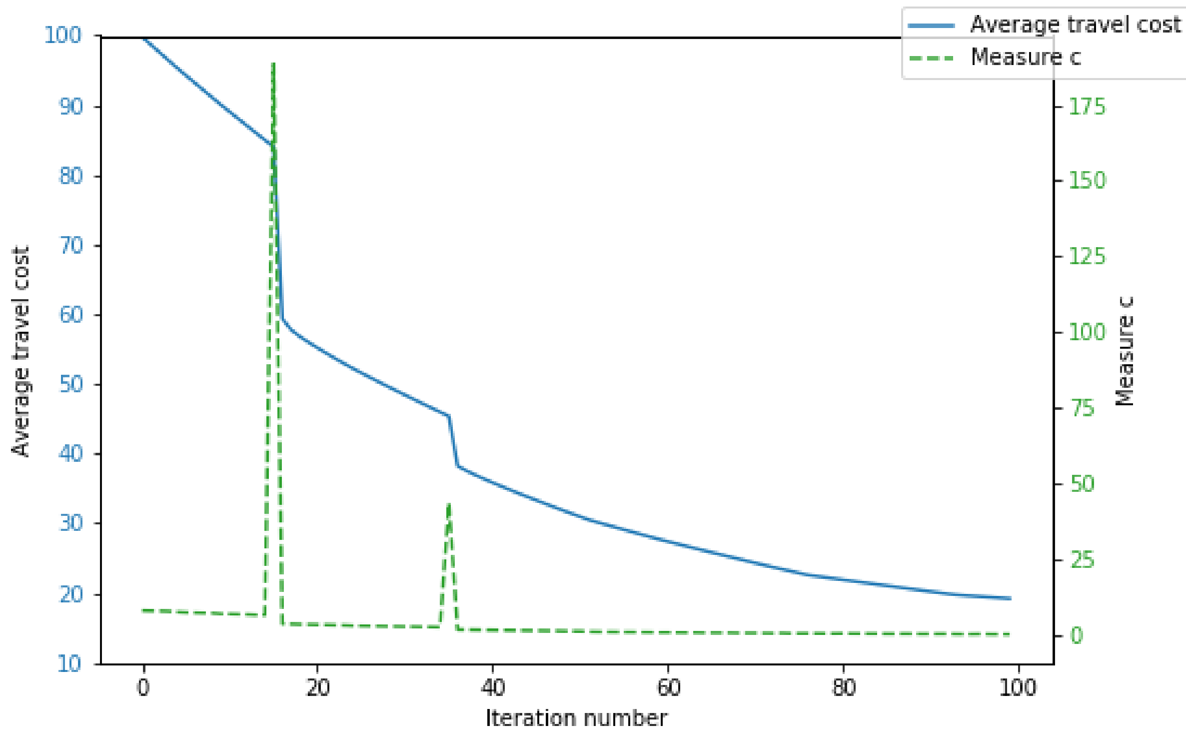

Figure 7: Correlation between such sharp changes in the average cost and the spikes observed in measure c for Nguyen-Dupuis' network at a demand per O-D pair of 450 vehicles and a learning rate of 1e-4.

c) Running times of the algorithms:

Table 1 compares the running times (in seconds) of different subtasks in the proposed algorithms for the two example networks. The simulation code is written in Python programming language using Numpy and Scipy packages and all the simulations were run on a 64-bit Intel Core i5-6500 3.2 GHz Quad-Core processor. For the purpose of comparison, the total demand between each O-D pair in both the networks is assumed to be 1800 vehicles. Each iteration takes less than 1 second in the case of Ziliaskopoulos network and a little more than 2 seconds is needed for Nguyen-Dupuis network. The complexity of the network and the demand level affect the number of iterations taken by the algorithm to converge, thereby increasing the running time.

Table 1
Comparison of the average running time (in seconds) of different subtasks in the proposed algorithms

Task	Ziliaskopoulos network	Nguyen-Dupuis network
Initialization	0.00	0.0025

Simulation	0.31	1.01
Calculation of average travel costs	0.03	0.11
Calculation of marginal costs	0.13	0.55
DUE quadratic program	0.092	0.48
DSO quadratic program	0.095	0.53

Conclusion and future work:

This paper formulates user equilibrium and system optimum problems within a generalized node-based DTA framework with an embedded cell transmission model for a traffic network with multiple origin-destination pairs. Both departure time choices at each origin and turning choices at each diverging intersection are incorporated in the models. Since the framework is node-based, the enumeration of paths is avoided and the efficiency of the solution algorithms is significantly improved. The contributions made by the present work can be listed as follows:

- Proposal of a node-based cell transmission model that satisfies the FIFO principle at link-level, i.e., the vehicles exit any given link in the same order as they entered it.
- Embedding the proposed CTM in a complementarity formulation for user equilibrium DTA with simultaneous departure time and route choices. Since the model is node-based, the route choice is made collectively by the individual turning choices of the traffic at the diverging intersections.
- Embedding of the proposed CTM in a new node-based system optimum DTA model with simultaneous departure time and route choices.
- Development of a time-dependent shortest path algorithm to efficiently compute average travel costs, which includes travel time and schedule delay components.
- Development of an efficient, backpropagation algorithm to compute marginal costs with travel time and schedule delay components.
- Adaptation of the projection algorithm to solve the two problems and a discussion of their results.

Simplifying assumptions have been made at different points in the proposed models and their realism can be improved in the future by modifying them appropriately. For example, the real traffic networks can be too complicated to be fully represented by the types of intersections possible in the CTM. And the computation techniques developed in this paper are fairly generalizable to any new and improved CTMs. In addition, the proposed models could be used in the standard transportation network problems like traffic signal optimization, congestion pricing, etc. As both UE-DTA and SO-DTA models share a similar framework, they could be used in studying the network efficiency problem and developing mechanism design tools improve the performance of a given network.

References:

1. Arnott, R., De Palma, A., & Lindsey, R. (1993). Properties of dynamic traffic equilibrium involving bottlenecks, including a paradox and metering. *Transportation science*, *27*(2), 148-160.
2. Bar-Gera, H. (2002). Origin-based algorithm for the traffic assignment problem. *Transportation Science*, *36*(4), 398-417.
3. Carey, M., Bar-Gera, H., Watling, D., & Balijepalli, C. (2014). Implementing first-in–first-out in the cell transmission model for networks. *Transportation Research Part B: Methodological*, *65*, 105-118.
4. Daganzo, C.F., 1994. The cell transmission model: A dynamic representation of highway traffic consistent with the hydrodynamic theory. *Transportation Research Part B: Methodological*, *28*(4), pp.269-287.
5. Daganzo, C.F., 1995. The cell transmission model, part II: network traffic. *Transportation Research Part B: Methodological*, *29*(2), pp.79-93.
6. Doan, K., & Ukkusuri, S. V. (2012). On the holding-back problem in the cell transmission based dynamic traffic assignment models. *Transportation Research Part B: Methodological*, *46*(9), 1218-1238.
7. Doan, K. and Ukkusuri, S.V., (2015). Dynamic system optimal model for multi-OD traffic networks with an advanced spatial queuing model. *Transportation Research Part C: Emerging Technologies*, *51*, pp.41-65.
8. Gentile, G. (2014). Local User Cost Equilibrium: a bush-based algorithm for traffic assignment. *Transportmetrica A: Transport Science*, *10*(1), 15-54.
9. Han, L., Ukkusuri, S., & Doan, K. (2011). Complementarity formulations for the cell transmission model based dynamic user equilibrium with departure time choice, elastic demand and user heterogeneity. *Transportation Research Part B: Methodological*, *45*(10), 1749-1767.
10. Karoonsoontawong, A., & Waller, S. T. (2010). Integrated network capacity expansion and traffic signal optimization problem: robust bi-level dynamic formulation. *Networks and Spatial Economics*, *10*(4), 525-550.
11. Long, J., Gao, Z. and Szeto, W.Y., 2011. Discretised link travel time models based on cumulative flows: formulations and properties. *Transportation Research Part B: Methodological*, *45*(1), pp.232-254.
12. Merchant, D. K., & Nemhauser, G. L. (1978). A model and an algorithm for the dynamic traffic assignment problems. *Transportation science*, *12*(3), 183-199.
13. Nie, X. J., (2003). The study of dynamic user-equilibrium traffic assignment. Ph.D. Thesis, University of California, Davis.
14. Nie, Y. M. (2010). A class of bush-based algorithms for the traffic assignment problem. *Transportation Research Part B: Methodological*, *44*(1), 73-89.
15. Ramadurai, G., Ukkusuri, S. V., Zhao, J., & Pang, J. S. (2010). Linear complementarity formulation for single bottleneck model with heterogeneous commuters. *Transportation Research Part B: Methodological*, *44*(2), 193-214.

16. Shen, W., Nie, Y., & Zhang, H. M. (2006). Path-based system optimal dynamic traffic assignment models: formulations and solution methods. In *2006 IEEE Intelligent Transportation Systems Conference* (pp. 1298-1303). IEEE.

17. Shen, W., & Zhang, H. M. (2009). On the morning commute problem in a corridor network with multiple bottlenecks: Its system-optimal traffic flow patterns and the realizing tolling scheme. *Transportation Research Part B: Methodological*, *43*(3), 267-284.

18. Szeto, W. Y., & Lo, H. K. (2004). A cell-based simultaneous route and departure time choice model with elastic demand. *Transportation Research Part B: Methodological*, *38*(7), 593-612.

19. Ukkusuri, S.V., Han, L. and Doan, K., 2012. Dynamic user equilibrium with a path based cell transmission model for general traffic networks. *Transportation Research Part B: Methodological*, *46*(10), pp.1657-1684.

20. Ziliaskopoulos, A. K. (2000). A linear programming model for the single destination system optimum dynamic traffic assignment problem. *Transportation science*, *34*(1), 37-49.